***Spring 2004* MEMS ALLIANCE SPECIAL TOPICS SYMPOSIUM**
***MEMS in Homeland Security, Defense, and Aerospace Applications***

****Schedule of Events***

## Monday March 29, 2004

| | |
|---|---|
| 8:00 - 9:00 | **~ Registration and Continental Breakfast ~** |
| | *Session Chair, Michael Gaitan |
| 9:00 - 9:40 | ***Invited Speaker Chris Foster**, MD Department of Business and Economic Development* |
| 9:40 - 10:20 | ***Invited Speaker John Butler**, National Institute of Standards and Technology* |
| 10:20 - 10:35 | **~ Break ~** |
| 10:35 - 10:55 | 04-01. **Applications of MEMS in Homeland Security: Detection Technologies for Weapons of Mass Destruction** David J. Nagel |
| 10:55 - 11:20 | 04-16. **Microfluidic Focusing Methods: Prospects for High-Sensitivity Detection and Separation of Biological and Chemical Warfare Agents** David Ross |
| 11:20 - 11:45 | 04-15. **uCantilever Gas Sensors with Custom Drive Electronics for Testing & Handheld Applications** Stanley Stepnowski, Eric Houser, R. Andrew McGill |
| 11:45 - 12:10 | 04-09. **MEPS – MEMS Electrochemical Power Supplies: Low-Cost Integrated Power for Homeland Security and Defense Microsystems** Charles Lakeman, Patrick Fleig, and Jenniffer DeGreeff |
| 12:10 - 1:20 | **~ Lunch ~** |
| | *Session Chair, Ron Polcawich |
| 1:20 - 2:00 | ***Invited Speaker R. Andrew McGill**, Naval Research Laboratory* |
| 2:00 - 2:25 | 04-12. **In situ Measurements of Temperature and Species Concentration in a Microscale Combustion Reactor** Scott Heatwole, Christopher Cadou, and Steven Buckley |
| 2:25 - 2:50 | 04-02. **The MEMS Flux Concentrator: A device for minimizing the effect of 1/f noise** A.S. Edelstein,[1*] Jeff Pulskamp,[1] Michael Pedersen,[2] and William Bernard[2] |
| 2:50 - 3:00 | **~ Break ~** |
| 3:00 - 3:25 | 04-19. **3d Silicon MEMS Fabrication Using Gray-Scale Lithography and Deep Reactive Ion Etching** C.M. Waits, B. Morgan, and R. Ghodssi |
| 3:25 - 3:50 | 04-17. **Electrostatically Actuated Resonant Microcantilever in CMOS Technology for Gas Sensor Applications** Ioana Voiculescu, Mona Zaghoul, R. Andrew McGill, Eric Houser, Stanley Stepnowski, Evgueni Sokolovski, and Gary Fedder |
| | *Poster Chair, Samara Firebaugh |
| 3:50 - 7:00 | **~ Poster Session and Evening Reception ~** |

## Tuesday March 30, 2004

| | |
|---|---|
| | *Session Chair, Robert Osiander |
| 8:30 - 9:15 | ***Invited Speaker Thomas George**, Jet PropulsionLaboratory* |
| 9:15 - 9:40 | 04-04. **MEMS-based Magnetometer Manufactured in 0.35um SiGe BiCMOS Process** Eli Richards and Dennis Wickenden |
| 9:40 - 10:10 | 04-07. **Wireless Communications Systems for MEMS Sensor Arrays** Matthew Bevan, Wolfger Schneider, and Kenneth Wright |
| 10:10 - 10:35 | 04-14. **Design and Packaging Considerations for a Microelectromechanical Satellite Thermal Control Device** Matthew A. Beasley and Samara L. Firebaugh |
| 10:35 - 10:50 | **~ Break ~** |
| 10:50 - 11:15 | 04-10. **Fuel- Air Mixing Challenges in Micro-Power Systems** Kiran Dellimore and Christopher Cadou |
| 11:15 - 11:40 | 04-20. **Development of MEMS-based Micronozzles for Gas Separation** Sheng Li, Carl B. Friedhoff, Robert M. Young, and Reza Ghodssi |
| 11:40 - 12:05 | 04-06. **Novel MEMS Stirling Cooler** Keith Rebello, Matthew Moran, Danielle Wesolek, Bruk Berhane, and Ann Garrison Darrin |
| 12:05 - 1:15 | **~ Lunch ~** |
| | *Session Chair, Brian Jamieson |
| 1:15 - 2:00 | ***Invited Speaker Kensall Wise**, University of Michigan* |
| 2:00 - 2:25 | 04-03. **Fabrication of MEMS-Based Microshutter Arrays for Optical Transmission Selection** Bernard Lynch, David Franz, R.G. Hu, M.D. Jhabvala, C.A. Kotecki, M.J. Li, H. Oh, and Y. Zheng |
| 2:25 - 2:35 | **~ Break ~** |
| 2:35 - 2:40 | **~ Award Best Poster ~** |
| 2:40 - 3:05 | 04-08. **A Micro- Machined Flat Plasma Spectrometer (FlaPS)** Danielle Wesolek, John L. Champion, Fred A. Herrero, Robert Osiander, Roy L. Champion, and Ann Darrin |
| 3:05 - 3:30 | 04-11. **Effect of Structural Heat Conduction on Flame Propagation and Power Density in Micro Combusters** Timothy Leach, Christopher Cadou, and Gregory Jackson |

***Schedule may be changed based on the discretion of the committee.**
**www.memsalliance.org**

# POSTERS

04-05. Shear Stress Sensors for Turbulence Control -Sateesh S. Bajikar[1], Michael A. Scott[2] and Edward E. Adcock[2—] **POSTER- NASA GSFC**
Sateesh Bajikar [Sateesh.Bajikar@gsfc.nasa.gov]

04-13. Interferometric Optical Detection in a Silicon on Saphire CMOS Process- Francisco Tejada and Andreas Andreau- **POSTER- JHU**
Francisco Tejada [ft1@olympus.ece.jhu.edu]

04-18. MEMS TACTILE ACTUATORS FOR PILOT ORIENTATION SYSTEMS-James E. Smith, John D. Roth, Samara L. Firebaugh – **POSTER- USNA**

04-21. Maskless Fabrication of JFETs via Focused Ion Beams- Anthony J. De Marco, John Melngailis- **POSTER-UMD;** Anthony J. De Marco [adeptus@wam.umd.edu]

04-22. Use of Focused-Ion-Beam Technology for MEMS Devices in Space Applications- Wen-Hsien Chuang, Rainer K. Fettig, and Reza Ghodssi- **POSTER-UMD**

04-23. InP-Based Optical Waveguide MEMS Switch Marcel W. Pruessner, Madhumita Datta, Reza Ghodssi-**POSTER-UMD**

04-24. BCB-Based MEMS Technology
Nima Ghalichechian, Alireza Modafe, and Reza Ghodssi - **POSTER-UMD**

04-25. Biolabs on a Chip: Design, Fabrication, and Charectorization- Yingkai Liu and Elizabeth Smela- **POSTER-UMD**

04-26. Mustard Gas Sensor- Kehinde Alli **POSTER-UMD**

04-27. DRIE Trenches and PDMS Cap for Electro-Osmotic Flow -Anthony Downs **POSTER-UMD**

04-28. Design and Fabrication of a Biodegradable Microsyringe - Jeffrey Krotosky **POSTER-UMD**

04-29. A micromachined variable capacitor with increased tuning range for use in an all-pass filter- Carlos Martinez **POSTER-UMD**

04-30. In-Plane Torso Joint and Actuator for Ant-Like Robot -Mario Urdaneta **POSTER-UMD**

04-31. Fabrication of a Multi Polymeric Bio-Integrable Transdermal Sampling Device- A.P. Gadre, Y.N. Srivastava, N. Ganesan, M. Paranjape, and J.F. Currie- **POSTER-GU**

04-32. Microgripper for an Insect-Like Microrobot -Saifa Hasin

# Applications of MEMS in Homeland Security: Detection Technologies for Weapons of Mass Destruction

David J. Nagel
The George Washington University
2033 K Street NW Suite 340J, Washington DC 20052
202-994-5293 (Office) 202-994-5505 (FAX) nagel@gwu.edu

The most valuable commodity for protection of a country and its people is adequate and timely information. The information that is needed to forestall attacks can be obtained by a variety of intelligence operations. Reliable information from humans is critical, but difficult to obtain. Interception of communications and acquisition of images, especially from satellites, are also heavily used techniques for homeland defense. The employment of instrumental detection technologies for the materials and devices that make up weapons of mass destruction is also very important. Such technologies increasingly involve and rely upon the use of MEMS.

Preventing the acquisition, manufacture, transport and use of weapons of mass destruction (WMD) is of primary importance for homeland security. WMD are of great interest not only because of their dramatic potential for damage to people and things. Also, they can be employed by a relatively small number of attackers in a very wide variety of scenarios. Detection technologies can be used during many of the phases in the life cycle of a WMD to provide information of varying specificity. Their primary limitation is the requirement, in most cases, for the detection instrument to be quite close to the material or device of interest.

Four types of materials for WMD are susceptible to detection by a wide variety of commercially available and developmental instruments: nuclear materials, explosives, chemical agents and biologicals. Nuclear materials are key to both nuclear devices and radiation dispersion weapons ("dirty bombs"). Explosives, which are part of both these types of weapons, can be incredibly damaging by themselves. The Murrah Building explosion in Oklahoma City is a prime example. Chemical agents, and many industrial chemicals, can cause great damage to humans and other animals. The Tokyo subway attack with Sarin and the accident in Bhopal, India, provide witness to this problem. Viruses, bacteria, spores and toxins are all of great interest, with the recent anthrax attacks in the U. S. being a well-known example of a biological attack.

**Nuclear materials** of interest fall into two primary categories. The first consists of weapons grade uranium and plutonium, which can be made into nuclear devices. The second includes radioactive isotopes of cesium, cobalt, iridium and strontium, which are employed for a variety of industrial and medical purposes. All these radioactive materials are candidates for use in radiation dispersion devices. Gamma rays and neutrons from such materials will penetrate nearby solids, and the atmosphere for distances up to several meters. However, such radiations will also go through small detectors, rendering them inefficient. Hence, MEMS generally have a limited role to play in homeland security for the detection of nuclear materials. The few current and prospective roles of MEMS in the detection of nuclear materials will be cited.

**Explosives** can be made from hundreds of energetic materials. Of greatest interest are about ten materials, the so-called high explosives. They generally contain molecules with sizes and affinities sufficient to suppress evaporation. Hence, the explosives of most interest for fighting terrorism have relatively low vapor pressures, and they remain as particles for long times. Most detection technologies for explosives require swiping a surface of interest to acquire such particles for their insertion into an instrument, followed by vaporization and measurement. The systems now on the market for explosives detection usually do not involve MEMS. However, a great deal of effort is currently going into the development of both (a) micro-machined concentrators to acquire enough molecules for measurement and (b) a wide variety of MEMS sensors to detect them. Examples of such devices will be provided to illustrate the potential impact of MEMS on this part of homeland security.

The number of **chemical agents**, specifically designed to kill or harm humans, and the industrial chemicals that are potentially dangerous, is also very large. In this arena, the focus is on about three dozen chemicals, including pulmonary, nerve, blood and blister agents. Large stockpiles of such materials still exist in the world. Chemical agents are somewhat easier to detect than explosives because they have higher vapor pressures, a fact that also makes their dispersion potentially very dangerous. A wide variety of instruments for detecting chemical agents is already on the market and many systems are being developed. MEMS are central to many of the instruments now in hand or in sight. Diverse nano-materials are also under development for the detection of dangerous chemicals. Chemical detection instruments are important for commercial reasons as well as for homeland security and military operations. Several examples of available and developmental techniques for concentrating and detecting chemical agents and other dangerous chemicals using micro- and nano-technologies will be surveyed.

The detection of harmful **biological materials** suffers from two major problems. The first is sampling. These particles are dispersed in a large volume of air with a background of many inorganic and organic particles. Acquiring and sorting of the bacteria, spores or viruses from such backgrounds varies from very challenging to impossible. The second major difficulty is to actually detect the materials of interest with enough specificity. Bio-detection is the least advanced of detection techniques for materials and components of WMD. The devices now on the market for bio-detection are relatively limited. However, many concepts are being vigorously developed for bio-sensors. This effort is driven in part by diverse commercial and medical applications of handheld detection instruments for bio-materials. Examples of bio-detection instruments based on micro-and nano-technologies will be shown.

The employment of MEMS-based and other detectors for WMD materials is set in a larger context, which includes the flow of information from such instruments to decision makers. Some of the wider challenges of using such instruments will be noted.

This presentation is based on a study entitled "Detection Technologies for Weapons of Mass Destruction" funded by the National Defense University and conducted by David J. Nagel, Gary W. Phillips (Georgetown University) and Timothy Coffey (National Defense University).

# Microfluidic Focusing Methods: Prospects for High-Sensitivity Detection and Separation of Biological and Chemical Warfare Agents

David Ross, Karin Balss, Heather Begley, Alyssa Henry, Peter Howell, Laurie Locascio, Ted Maliaris, Kim Olsen, Karen Phinney, Mike Tarlov, and Wyatt Vreeland

National Institute of Standards and Technology
100 Bureau Dr.
Gaithersburg, MD 20899
david.ross@nist.gov

The most commonly used separation methods in microfluidics (such as capillary electrophoresis (CE) or capillary electrochromatography (CEC)) separate different molecular species by causing them to move with different velocities through a small diameter microchannel or capillary. A plug of mixed analyte is introduced at the beginning of the channel and the different components are separated as they move to the end of the channel where they are detected. These types of separations suffer from poor detection limits because of the small amounts of sample typically injected into the separation channel and the dispersion of the analyte peaks as they move down the channel.

Focusing methods separate analytes by causing them to be spatially localized or focused at different points along a microchannel. Because of their combination of high-resolution separation with simultaneous concentration enhancement, focusing methods can provide a powerful mode of separation with very low detection limits. Currently, the only focusing mode technique that is widely used and available is isoelectric focusing (IEF). Although IEF is an extremely high performance separation technique for proteins and peptides, it is, unfortunately, applicable only for proteins and peptides.

As part of the NIST microfluidics project, we are working on a number of new, alternative separation methods that can provide the kind of high performance inherent to focusing techniques and that are applicable to a broader range of analyte types. The new methods developed at NIST include temperature gradient focusing (TGF) for the focusing and separation of all types of charged analytes and micellar affinity gradient focusing (MAGF) for focusing and separation of uncharged and/or hydrophobic analytes.

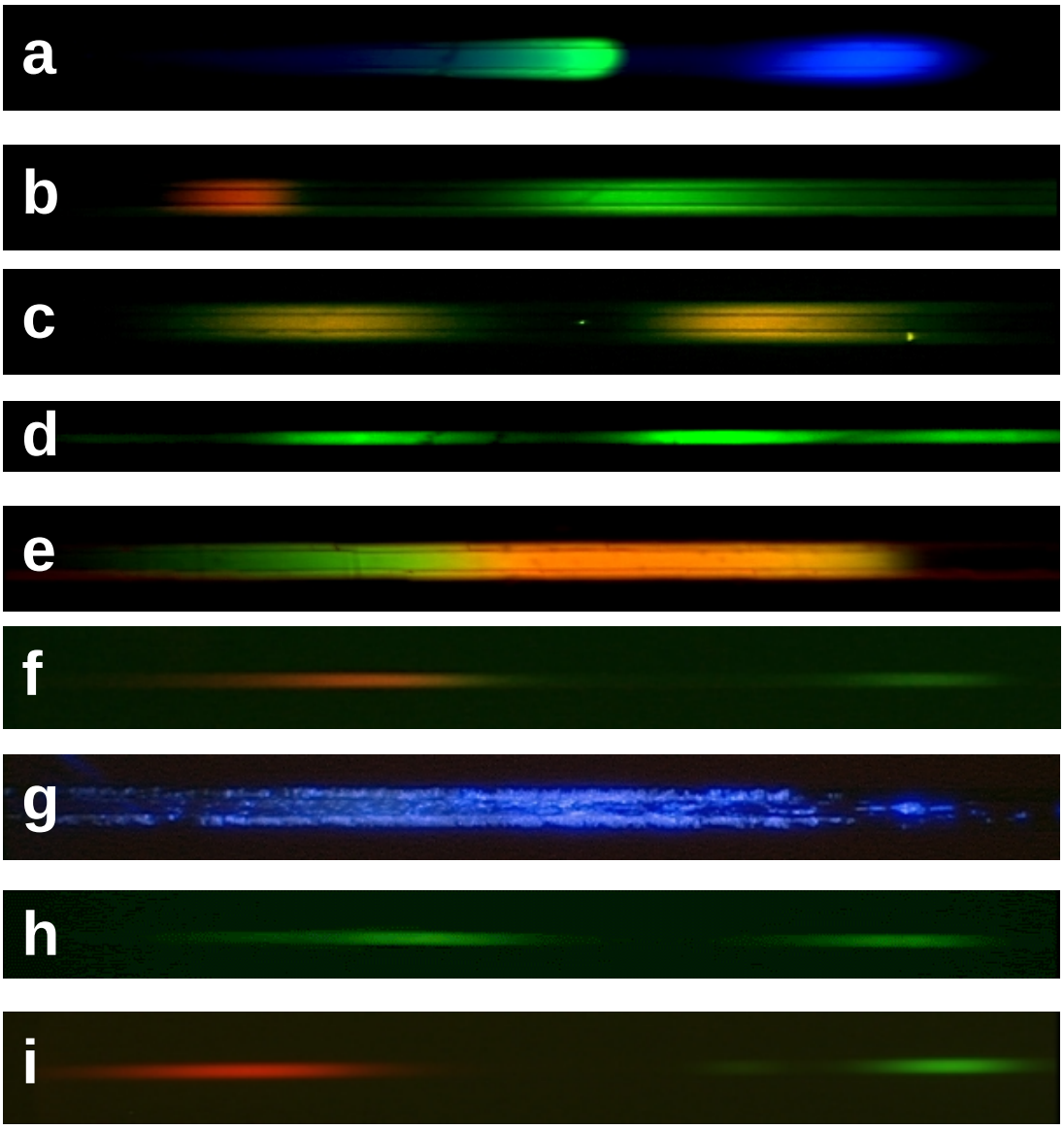


New microfluidic focusing methods developed at NIST are capable of simultaneous separation and concentration enhancement of a variety of different analytes. Temperature gradient focusing (TGF) has been shown to be effective with all types of ionic analytes such as small dye molecules (a), amino acids (b-c), proteins (d), DNA (e-f), large particles and cells (g), and for chiral separations (h). Micellar affinity gradient focusing (MAGF) provides a focusing mode analog to MEKC for the concentration and separation of hydrophobic analytes (i).

# μCantilever Gas Sensors with Custom Drive Electronics for Testing & Handheld Applications

Stanley Stepnowski, Eric Houser, R. Andrew McGill
Naval Research Laboratory, Code 6365, Washington, D.C. 20375-5345
(202) 404-1964 (Tel); (202) 767-5301 (Fax); stan@ccf.nrl.navy.mil

Evgueni Sokolovski, Jennifer Stepnowski
Nova Research, Inc., Alexandria, VA 22308

Ioana Voiculescu
George Washington University, Mechanical and Aerospace Engineering, Washington, DC 20052

David Hedden, ThomasThundat
Oak Ridge National Laboratory, Life Sciences Division, Oak Ridge, TN

There is an acute need for highly sensitive, accurate, and rapid detection techniques for explosives, chemical agents, and toxic industrial chemicals. In order to practically monitor for these illicit materials, portable trace detection techniques are required. Current detection technologies that are commercially available for these application areas are typically considered expensive (> $10,000), large (shoebox), and power hungry (> 5 W). In order to provide improved capabilities, detection techniques are desired which offer similar or improved trace detection, but with a much smaller system form factor, much lower power requirements, and a much less expensive production cost. It is therefore attractive to consider the use of micromachined technologies that pave the way for on-chip electronics at lower costs and higher production yields.

As an example micromachined transducer technology, a number of microcantilever devices have been investigated at the Naval Research Laboratory (NRL), with devices ranging from off the shelf cantilevers with custom designed electronics to custom cantilever designs and associated electronics.

Two main microcantilever designs have been explored including (i) a COTS Piezolever™ device incorporating a single piezoresistor that is driven acoustically, and (ii) a custom design that is electrostatically actuated and piezoresistively sensed.

## (i) Acoustically Actuated Sensor

A Piezolever™ contact mode self-sensing cantilever from Veeco Inc. was operated acoustically by driving it with a piezoelectric speaker attached to the underside of the cantilever mounting. The cantilever was held in place with metal clips, providing mechanical coupling and electrical contact. External resistors completed a Wheatstone bridge circuit connected to an instrumentation amplifier that produced a changing voltage output as a function of changing cantilever motion. Follow-on electronics were designed to further amplify, wave shape, and provide feedback to the actuation to form a closed-loop oscillator. In order to tune the resonant frequency of the cantilever, two main approaches were demonstrated including a tunable low pass filter to provide a varying phase shift and a variable threshold Schmitt trigger. Initial experiments were carried out with an open loop phase detector technique that formed the basis of the current circuit. Variations of this design were used to monitor polymer coating processes and

for experiments towards creating a hand-held detection system for trace monitoring of illicit materials. The breadboard electronics and sensor manifold developed is shown in Figure 1a, and an example data set for a vapor challenge test are shown in Figure 1b. Experimental results show that the device provided reversible frequency shift responses to dimethylmethylphosphonate (DDMP) and 2,4,6-trinitrotoluene (TNT) vapor at concentrations ranging from ppb to ppm levels.

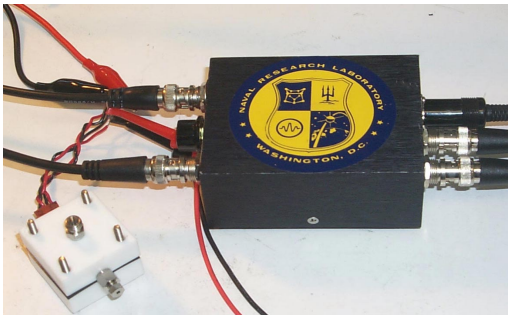

Figure 1a. Support electronics

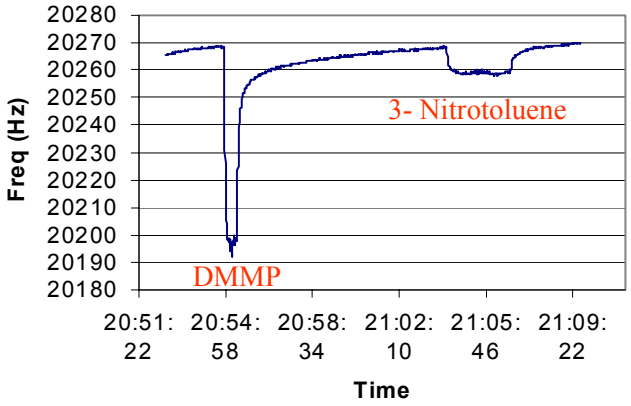


Figure 1b. Response to DMMP and 3-nitrotoluene

(i) Electrostatically Actuated Sensor

A silicon cantilever device designed in the Carnegie Mellon University (CMU) CMOS-MEMS process was operated electrostatically by driving it with a small varying AC signal imposed on a constant DC bias. The Austrian Microsystems (AMS) fabricated CMOS chip was mounted into a 40 pin DIP header for testing. In a similar fashion to the Piezolever™ technique, the signal from the on-chip Wheatstone bridge was amplified, phase shifted, and fed back by modulating the DC bias voltage to form a resonating system. The chip's array of cantilevers combined with the aforementioned circuit creates a self-contained system. Initially characterized with a spectrum analyzer, the self-contained apparatus was then used to eliminate laboratory support equipment. This portable device has been developed with a view towards further miniaturization into a palm-sized system.

The first generation breadboard electronics and sensor manifold developed is shown in Figure 2a, and an example data set for a DMMP vapor challenge are shown in Figure 2b. The data for an isothermal vapor concentration ramp demonstrated that the device provided reversible frequency shift responses as low as 20 ppb.

Figure 2a. Cantilever chip and support electronics

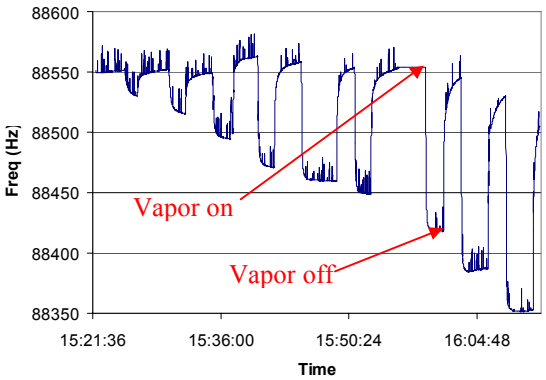


Figure 2b. Frequency response to increasing [DMMP]

# *MEPS – MEMS Electrochemical Power Supplies: Low-Cost Integrated Power for Homeland Security and Defense Microsystems*

Charles Lakeman, Patrick Fleig, and Jenniffer DeGreeff
TPL Inc., 3921 Academy Parkway North, NE, Albuquerque, NM 87109
Tel: (505) 342-4427 FAX: (505) 343-1797 e-mail: clakeman@tplinc.com

There is an important need for small-volume devices as sensors and advanced beacons (tag, track and locate, TTL), in covert applications. To remain undetected, these devices must have total volumes of less than (and sometimes much less than) $0.1cm^3$. While device technology (e.g., electronics and micromachines) has evolved to deliver these small-scale devices, similar developments in power technologies have not kept up. Even the smallest commercially available battery dwarfs these Lilliputian devices, and miniaturized power systems currently in development (e.g., thin film batteries) are unable to deliver useful capacities or power levels. **Sensors, covert wireless communications devices and TTL beacons for defense and homeland security applications, therefore, need small-scale, integrated energy sources.**

TPL has designed and built novel volumetric microbatteries and microsupercapacitors that can meet energy delivery needs for covert microsystems. These microdevices fully exploit the third dimension to maximize the energy and power densities for a given footprint. For example, our microbatteries with this geometry have capacities more than 500 times those of thin film devices with a similar footprint, and our microsupercapacitors have capacitance densities up to 12 times those of COTS devices.

***Microbatteries.*** Figure 1 shows the superior performance of our volumetric batteries compared with "conventional" thin film devices. Under a constant current drain of 128μA, these devices deliver a capacity to 1V of ~2mAhr and can last nearly 16 hours. By comparison thin film batteries with similar footprint (1.9mm x 1.3mm) delivered~3μAhr in 10 seconds. Figure 1 also shows that our microdevices deliver the desirable flat voltage discharge curve that is characteristic of Zn-air batteries.

***Microsupercapacitors***. A similar volumetric approach also improves the performance of microsupercapacitors (Table 1). Like batteries, supercapacitors are electrochemical devices; however, rather than generating a voltage from a chemical reaction, supercapacitors store energy by separating charged species in an electrolyte. As with COTS batteries, COTS supercapacitors are far too bulky for integration at the volume and length scales of interest for microsystems for covert applications. Our patented volumetric MEMS supercapacitor can be integrated on-chip to deliver high power density for transient pulse power needs.

***MEPS.*** A combination of a supercapacitor and a battery in parallel can extend battery life as, under high loads, most of the energy is delivered by the supercapacitor. The supercapacitor reduces the drain on the battery, which can be seen as less of a voltage drop under peak load (Figure 2).

***Summary.*** We have designed and built novel, volumetric, MEMS-scale electrochemical devices. By exploiting the z-dimension, these devices deliver high energy and power density for a given footprint, maximizing the operating lifetime. Combination of MEMS supercapacitors with MEMS batteries delivers high power pulses with a reduced size (volume and footprint) as well as improved voltage stability. The devices can be integrated on chip and deliver a unique solution to integrated power for covert devices for homeland security and defense.

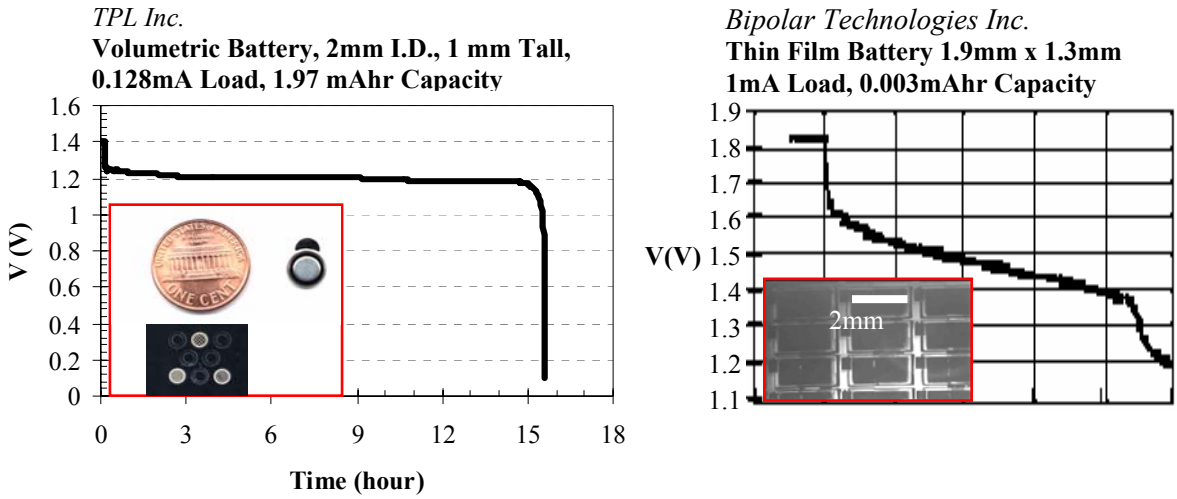


**Figure 1** Comparison of performance of TPL's *volumetric* microbatteries with thin film devices.

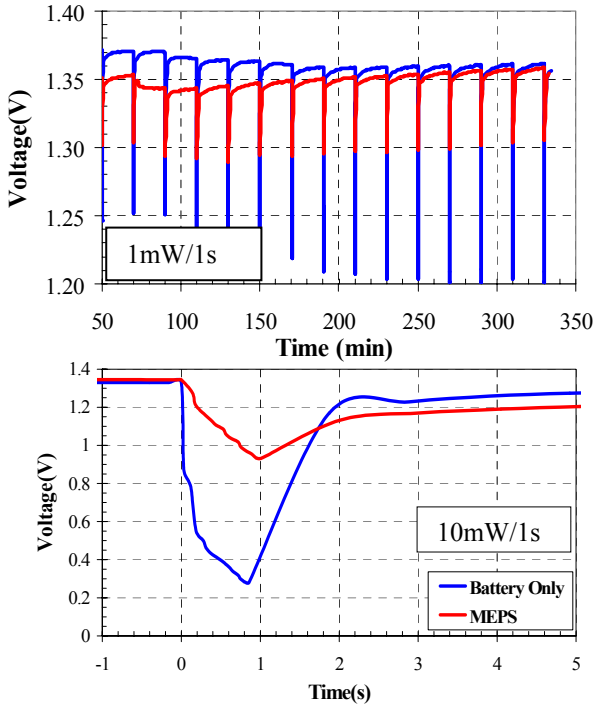


**Figure 2** Supercapacitor reduces voltage drop on high power pulse

**Table 1.** Performance of COTS supercapacitors and TPL's microsupercapacitors.

| Supercapacitor | Capacitance (F) | C* (mF/mm$^3$) | ESR (Ω) | Specific Power (mW/g) |
|---|---|---|---|---|
| ELNA DZ2R5D106 | 10.00 | 1.12 | 0.08 | 277 |
| Maxwell PC5 | 4.00 | 2.22 | 0.4 | 672 |
| Samsung DA5R5473V | 0.047 | 0.125 | 45 | 76.5 |
| **TPL aqueous** | **0.20** | **25.0** | **3** | **715** |
| **TPL organic** | **0.08** | **10.0** | **240** | **39.3** |

# *In situ Measurements of Temperature and Species Concentration in a Microscale Combustion Reactor*

**Scott Heatwole[1], Christopher P. Cadou[2], and Steven G. Buckley[3]**

[1] Department of Mechanical Engineering, University of Maryland, College Park, MD 20742

[2] Department of Aerospace Engineering, University of Maryland, College Park, MD 20742

Tel: 301.405.0829, Fax 301.314.9001, cadou@eng.umd.edu

[3] Department of Mechanical and Aerospace Engineering, University of California, San Diego, La Jolla, CA 92093-0411

## Abstract

Small combustion devices have recently generated substantial interest for powering micro-air vehicles (MAVs) and other sensor systems for national security applications. Combustion is as an attractive means of producing power because of the high energy density and ready availability of hydrocarbon fuels. Small-scale combustion studies have ensued in a variety of experimental configurations, but in most cases the combustion event cannot be directly monitored due to the combination of small sizes and limited optical or probe access to the combustion region. Such access is particularly important as the scale of these devices approaches or exceeds the traditional quenching limit, and reaction / structure coupling becomes increasingly significant.

This paper discusses a technique that allows direct observation of microscale combustion events occurring inside a silicon MEMS device. A small combustor fabricated from IR-transparent Si is used to demonstrate the viability of the technique. The combustor consists of two n-type Si wafers spaced 2-3 mm apart with a pre-mixed propane-air flame stabilized between them. The micro-combustor is installed in the optical path of a Fourrier-Transform Infrared Spectrometer (FTIR) which is used to collect spectra of $CO_2$, CO, and $H_2O$ through the combustor walls. The burner and its installation in the FTIR are illustrated in figure 1. Additional measurements indicate that it is also possible to observe spectral features of the fuel $C_3H_8$.

Local species concentration and temperature are computed from the spectra. Species concentration is determined from the overall strength of the absorption features. The basic idea behind the temperature measurement is that relative strengths of individual rotational features depend on temperature. A model representing the temperature dependence of CO rotational features is fit to CO spectra measured in the burner. The temperature corresponding to the best fit is taken to be the gas temperature. The spatial evolution of temperature and species concentration in the burner is determined by traversing the burner through the interrogation region of the FTIR. A sample axial temperature distribution determined using this technique is presented in figure 2.

Improved versions of this method may be useful for making in-situ measurements of temperature and species concentration in silicon MEMS-based micro-combustion devices. These, in turn will facilitate the development of reliable and efficient micro-power systems for MAVs.

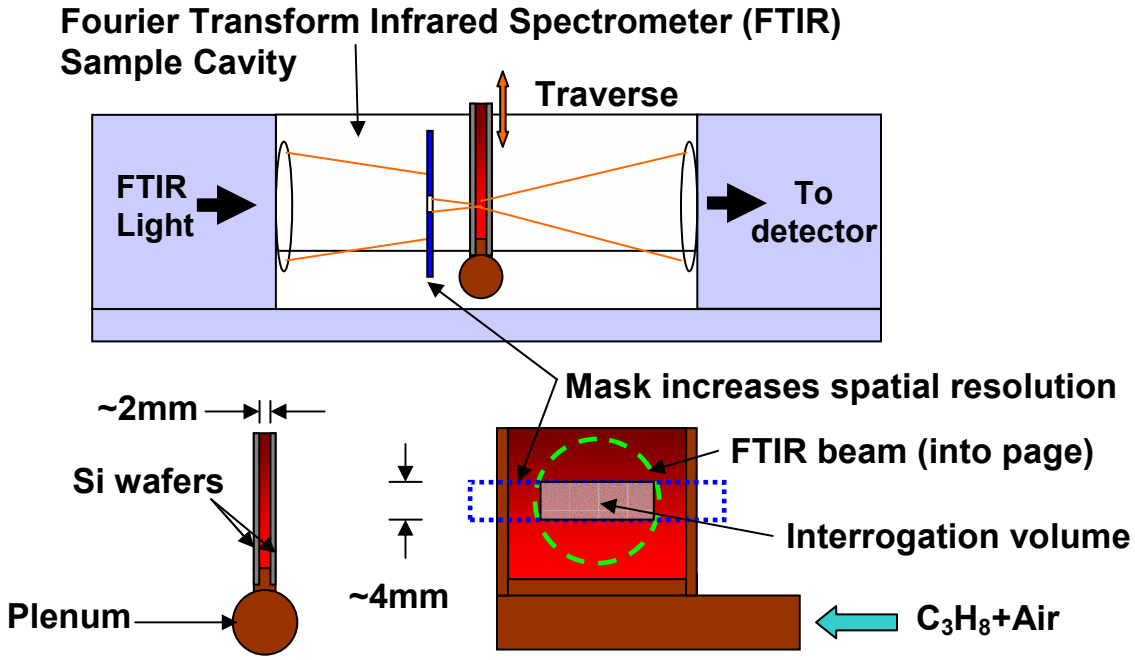


Figure 1: Schematic diagram of micro-combustor and FTIR

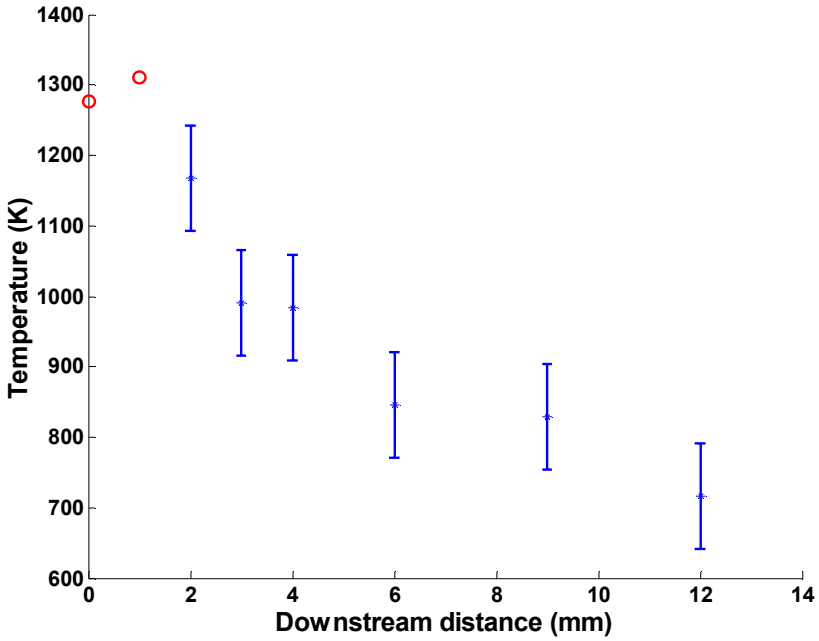


Figure 2. Axial temperature distribution in burner computed from CO spectra.

# The MEMS Flux Concentrator: A device for minimizing the effect of 1/f noise

A.S. Edelstein,[1*] Jeff Pulskamp,[1] Michael Pedersen,[2] and William Bernard[2]
1. Army Research Laboratory, Adelphi, MD 20783
2. MEMS Exchange, Reston, VA 20191

The low-frequency sensitivity of many magnetic sensors, such as AMR, GMR, spin dependent tunneling, and hall effect sensors, is decreased significantly by *1/f* noise. This decrease in sensitivity is a serious problem for many military applications where there is a need to detect the motion of vehicles and armed personnel. We have been working on a device, the MEMS flux concentrator, that mitigates the effect of 1/f noise by shifting the operating frequency of the sensor to higher frequencies. Often magnetic sensors are placed between soft magnetic materials called flux concentrators that multiply the magnetic field. In the present device, the magnetic sensor, a GMR sensor, is also placed placed between the flux concentrators. What is new is that the flux concentrators are on MEMS flaps that are driven to oscillate so that the multiplication factor varies between 6 when the flaps are closest to one another and 2 when they are furthest apart. The field at the position of the sensor oscillates at a frequency $2f_r$ where $f_r$ is the normal mode resonant frequency for the two MEMS flaps to oscillate $180^o$ out of phase with one another. Thus, the device shifts the operating frequency above the frequency region where *1/f* noise dominates.

Operating MEMS structures have been successfully fabricated starting with SOI wafers. The device layer Si is 5 microns thick and the SiO2 is 1 micron thick. We found that it is essential that the device Si and the handle Si are well bonded to the $SiO_2$ in order to correctly etch the $SiO_2$ during the release stage without releasing the MEMS structure from the handle Si. The basic structure is shown in Fig. 1. The motion is driven by comb drives. The two MEMS flaps are connected by springs so that there is a normal mode in which the two flaps move in the plane $180^o$ out of phase with one another. The _ micron thick layer of permalloy, deposited on the MEMS flaps by sputtering, has the expected magnetic properties and does not warp the flaps by being too stressed. The GMR structure has been fabricated in test runs. Except for one area, all of the Si on the handle layer beneath the MEMS structure was removed by using DRIE from the backside of the wafer. The handle Si was not removed under the bridge that will support the GMR sensor. Removing the handle Si minimizes possible problems due to stiction. One can directly observe the normal mode resonances that occur at around 10 kHz. The moving portions of the device look blurred because of the motion. Figure 2 shows the amplitude on the motion of one of the devices as a function of frequency. One sees the lower frequency in phase normal mode and the higher frequency in $180^o$ out of phase motion normal mode. The fabrication of the complete device is in progress. We know of no obstacles in completing the fabrication of working devices that include the GMR sensor. Minimizing the effect of *1/f* noise can increase the sensitivity of magnetoresistance sensors by one to three orders of magnitude.

* Alan S. Edelstein, U.S. Army Research Laboratory, 2800 Powder Mill Rd., Adelphi, MD 20783-1197, Tel. No. 301-394-2162, FAX No. 301-394-4605, Edelstein@arl.army.mil

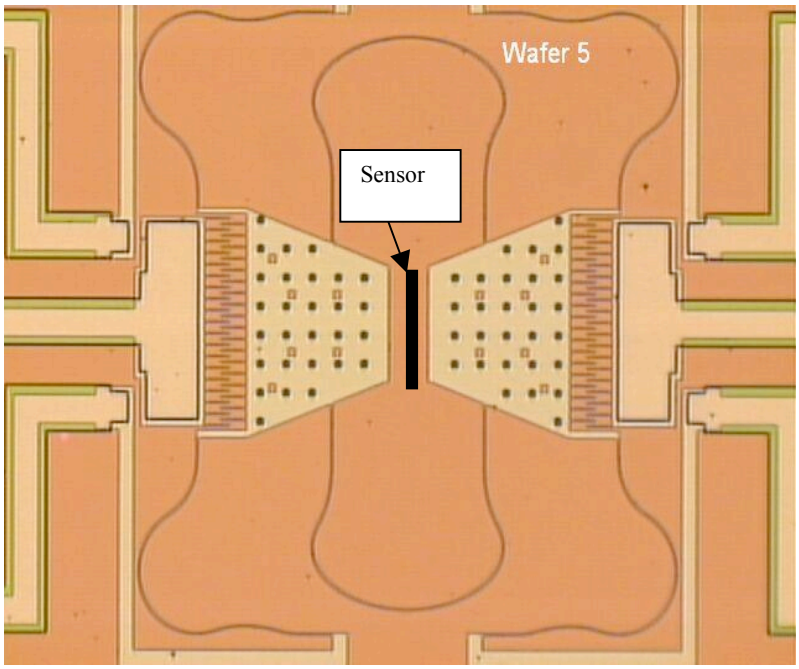


Figure 1. Picture of the MEMS flux concentrator

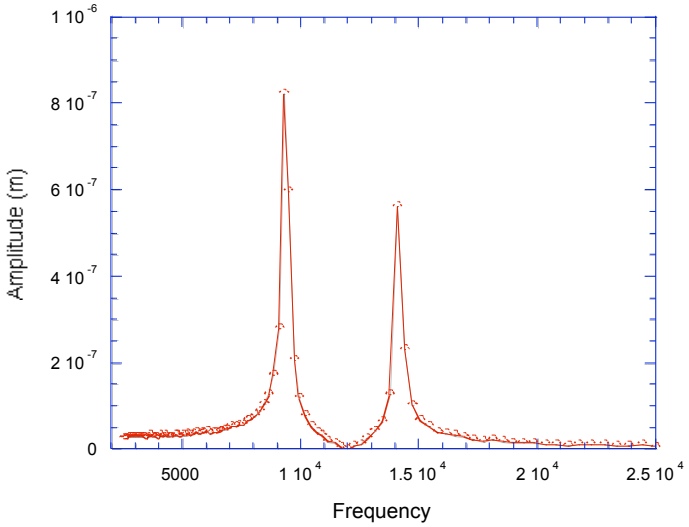


Figure 2. Amplitude of the motion versus frequency showing the two normal modes of one of the MEMS flux concentrator devices.

# 3D SILICON MEMS FABRICATION USING GRAY-SCALE LITHOGRAPHY AND DEEP REACTIVE ION ETCHING

C. M. Waits, B. Morgan, and R. Ghodssi

MEMS Sensors and Actuators Lab (MSAL)
Department of Electrical and Computer Engineering
Institute for Systems Research
University of Maryland, College Park

We report the successful fabrication and development of deep silicon structures with defined 3D profiles using gray-scale lithography and deep reactive ion etching (DRIE). Micro-electro-mechanical systems (MEMS) often require large lateral dimensions (>1mm) and depths (>20μm), previously not demonstrated using gray-scale technology. By the successful development of design techniques and tight processing controls gray-scale patterned photoresist with large lateral dimensions and tailored profiles are achieved. Additionally, DRIE recipes have been developed to extend gray-scale technology to greater depths where the selectivity between the photoresist structure and the final silicon structure defines a critical scaling factor (Figure 1). This is an enabling technology for air compression in power MEMS devices and high efficiency fresnel lenses for space applications [1-4].

Gray-scale optical masks were designed by varying the size of sub-resolution pixels, with a uniform center-to-center spacing, to locally modulate the amount of transmitted light. A calibration mask with varying pixel sizes was used to correlate the amount of light transmitted through the mask to the resulting photoresist heights from our lithography process. Photoresist height measurements were fit with a Gaussian curve, allowing for accurate design of future complex gray-scale structures. The Gaussian prediction for a mask-pitch of 2.8μm, and the resulting heights of our structures in AZ9245 photoresist, are shown in Figure 2. The equation for the Gaussian curve was then used to precisely design profiles in the photoresist.

Since the vertical dimensions of each silicon structure are entirely dependent upon etch selectivity during DRIE, precise selectivity control is paramount to the success of gray-scale technology. Experiments were conducted to obtain etch recipes with a wide range of etch selectivities. The key parameters used in tuning the selectivity were the silicon loading, electrode power, and a novel oxygen step added to the conventional Bosch process. An oxygen plasma between the etch step and the passivation step was used to control the photoresist etch rate during each cycle without greatly effecting the etched profile. Selectivities ranging from 14:1 to 115:1 have been achieved. This versatility in selectivity enables the lithography processing to remain constant while making process and design adjustments with only the DRIE step.

Two specific structures have been fabricated to demonstrate the versatility and applications of gray-scale technology. Figure 3 shows an 8mm micro-compressor structure made with >95 gray levels. A 2mm long gray-scale slope goes from an etch depth of 350μm at a radius of 2mm to an etch depth of 150μm at a radius of 4mm. This sloped micro-compressor will be part of a micro-gas turbine generator device and aims to increase engine cycle performance. Figure 4 shows a 1.6mm-diameter phase Fresnel lens made of 32 gray levels and etched 44μm into silicon. Ridge widths range from 260μm down to 30μm. This lens was designed to have a focal length of 118m for 8.4keV photons, appropriate for future testing at NASA's Marshall Space Flight Center. By fabricating this lens using gray-scale technology, the theoretical efficiency limit can be greatly increased, from 40.4% to over 95%, when compared to a traditional two level (binary) Fresnel lens.

Corresponding author: Dr. Reza Ghodssi, Department of Electrical and Computer Engineering, Institute for Systems Research, University of Maryland, A.V. Williams Bldg., Room 1357, College Park, MD 20742, USA. Tel: +1-301-405-8158; Fax: +1-301-314-9281; E-mail: ghodssi@eng.umd.edu.

*2004 MEMS Alliance Symposium on MEMS in Homeland Security, Defense and Aerospace Applications*
*March 29-March 30, 2004*

**References:**
[1] C.M. Waits, *et al*., *J. of Micromech. And Microeng.*, 13 (2003), pp. 170-177.
[2] R. Ghodssi, et al., *Proc. 2003 ARL CTA Symposium,* pp. 55-59, April 29 – May 1, 2003.
[3] B. Morgan, et al., *J. MEMS,* February 2004
[4] C. M. Waits, et al., *Sensors and Actuators* A, accepted January 2004.

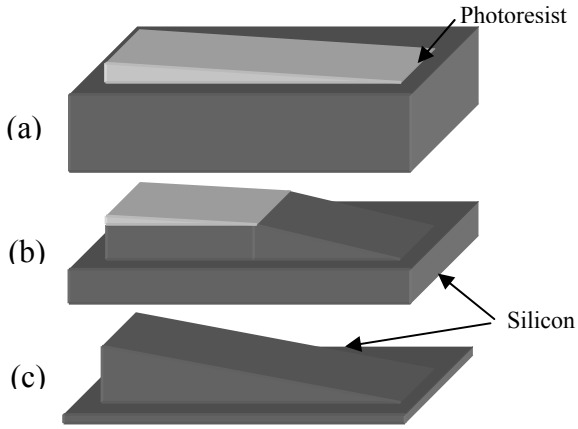


*Fig. 1: (a) Gradient photoresist structure on silicon, (b) pattern begins to transfer into the silicon with certain selectivity and (c) final structure in silicon retains lateral dimensions while vertical dimensions are amplified by the etch selectivity.*

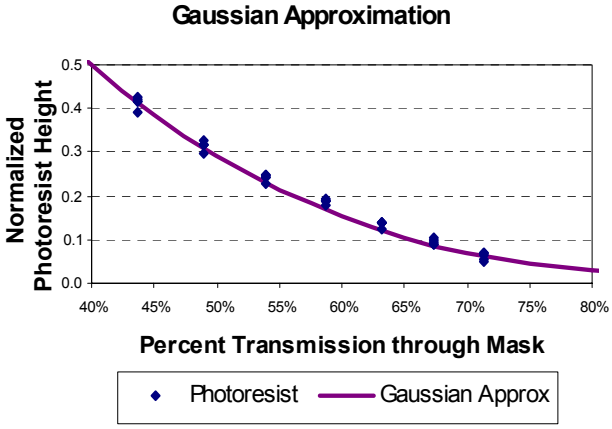


*Fig. 2: Gaussian tail approximation relating the normalized height in photoresist to the calculated percentage of light transmitted through the optical mask.*

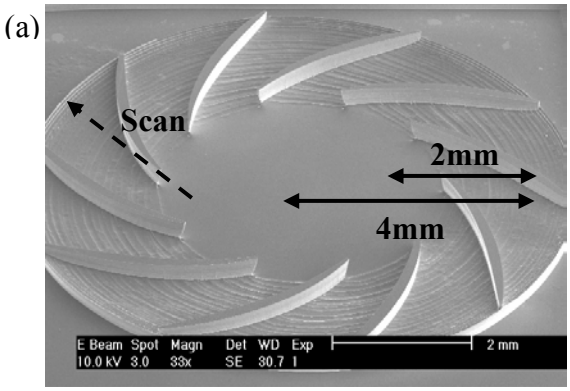


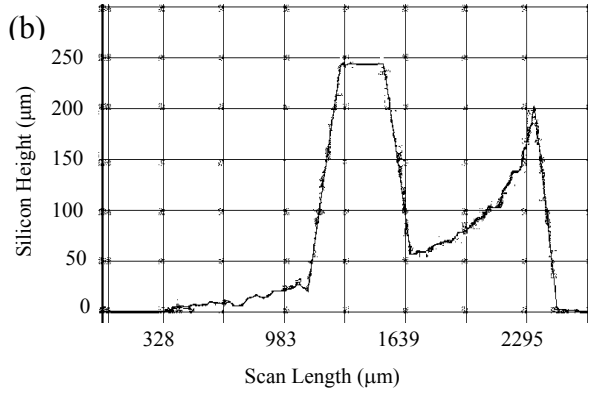


*Fig. 3: Sloped micro-compressor exhibiting >95 gray levels on a 2mm slope and a contact profilometer scan showing the peak of the slope to be 200 microns in silicon.*

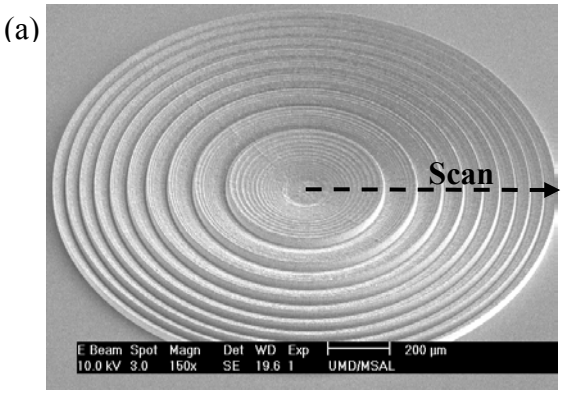


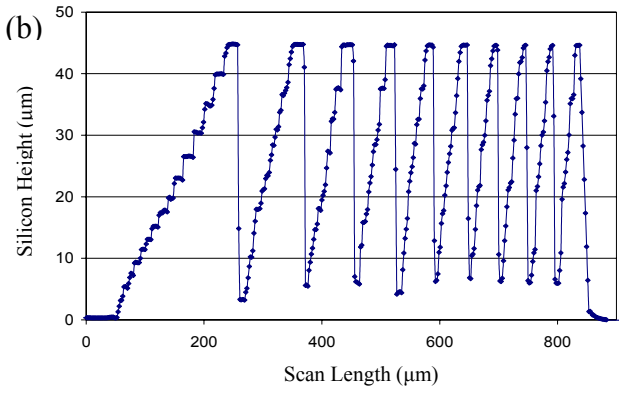


*Fig. 4: Phase Fresnel lens consisting of 10 profiled ridges for x-ray diffraction and refraction, where each ridge has a uniquely defined profile. Optical profilometer scan confirms the sloped profiles of the ridges.*

# Electrostatically Actuated Resonant Microcantilever In CMOS Technology for Gas Sensor Applications

Ioana Voiculescu, Mona Zaghloul, R. Andrew McGill, Eric J. Houser, Stanley Stepnowski, Evgueni Sokolovski, and Gary K. Fedder

The design, fabrication, and testing of a resonant cantilever in CMOS technology is presented. The resonant cantilever is demonstrated as a gas sensing device capable of monitoring hazardous vapors and gases at trace concentrations. The cantilever chemical sensor consists of two key components: a gas sorptive layer, e.g., a polymer, and the cantilever transducer, see Fig.1. The new design of the cantilever described here includes interdigitated fingers for electrostatic actuation, and a piezoresistive Wheatstone bridge design to read out the deflection signal. The reference resistors of the Wheatstone bridge are fabricated on auxiliary cantilevers that are immediately adjacent to the actuated device as shown in Fig.2. The whole device is fabricated using a 0.6 μm three metal, double poly CMOS (Complementary Metal Oxide Semiconductor) process, combined with subsequent micromachining steps [1].

The cantilever was coated with a custom NRL sorbent polymer [2], as shown in Fig. 3. The uptake of different gases is monitored as a shift in the device frequency, which is reversible if the gas-polymer chemical interactions are reversible. The cantilever gas sensor acts as a resonating microbalance, with mass increases normally leading to a decrease in the cantilever resonance frequency.

The tests were carried out by exposing the sensor to the nerve agent simulant, dimethylmethylphosphonate (DMMP) vapor at concentrations which were ramped from 43 mg/m³ to 0.1 mg/m³ in a repeated fashion. The cantilever sensor response as a function of DMMP concentration is shown in Fig. 4 and Fig. 5. The lowest DMMP concentration tested was 0.1 mg/m³ or 20 ppb. At this concentration, the signal frequency shift recorded was 40 Hz, with an estimated signal noise level of 10 Hz. The sensor time constant to 90% of signal was approximately 10 s.

These initial promising results were attained with a relatively simple design, fabricated in standard CMOS, which could offer an inexpensive option for production of a miniature chemical detector, with on chip electronics integrated to the cantilever.

Corresponding author:
Ioana Voiculescu, PhD student
George Washington University,
Mechanical and Aerospace Engineering
801- 22nd Street, NW
Washington, DC 20052
e-mail: ioana@gwu.edu
tel: 5713382048
fax: (202)767-5301

## REFERENCES

[1] G. K. Fedder, S. Santhanam, M. L. Reed, S. C. Eagle, D. F. Guillou, M. S. –C. Lu, L.R. Carley, "Laminated high-aspect-ratio microstructures in a conventional CMOS process", *Sensors and Actuators* A57, pp. 103-110, 1996

[2] E. J. Houser, D. L. Simonson, J. L. Stepnowski, R. A. McGill "Linear and Hyperbranched Hydrogen Bond Acidic Poly(silylene methylene)s for Chemical Sensor Applications" PMSE Preprints 2003, 88, 548

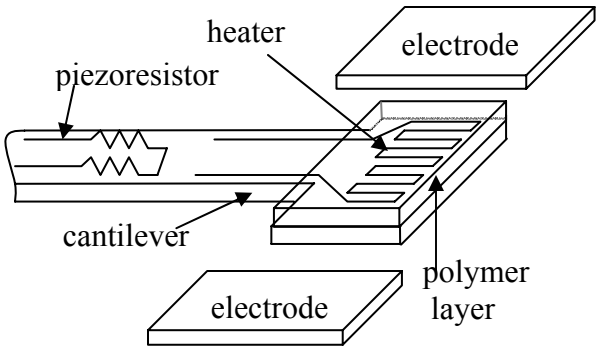


Fig.1. Microcantilever gas sensor. Electrodes are used for electrostatic actuation of the cantilever.

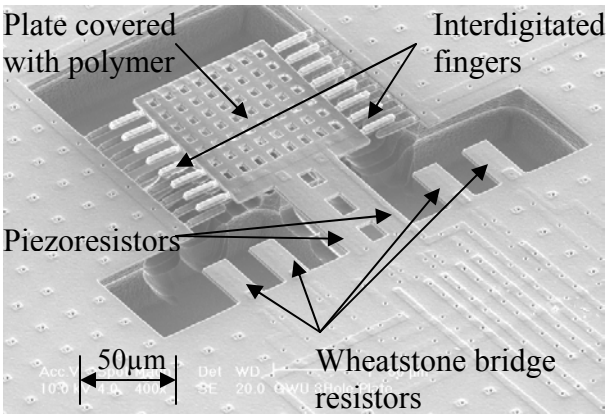


Fig. 2. Micrograph of Cantilever 6.

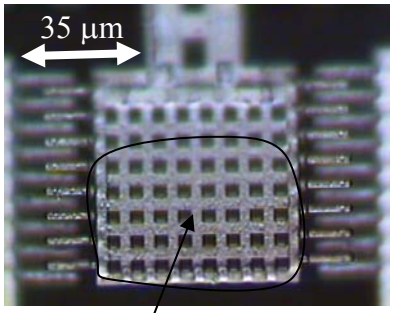


Fig.3. The polymer drop is deposited close to the cantilever tip. The device curling results in an image that is out of focus.

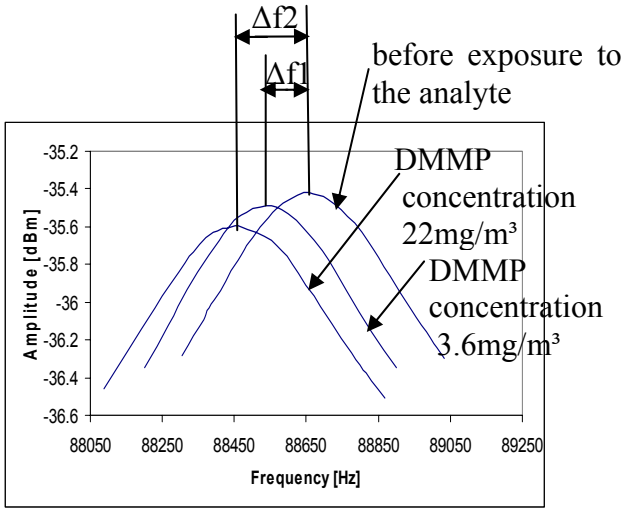


Fig.4. Cantilever response upon exposure to various DMMP concentrations. Frequency shifts are marked Δf1 and Δf2

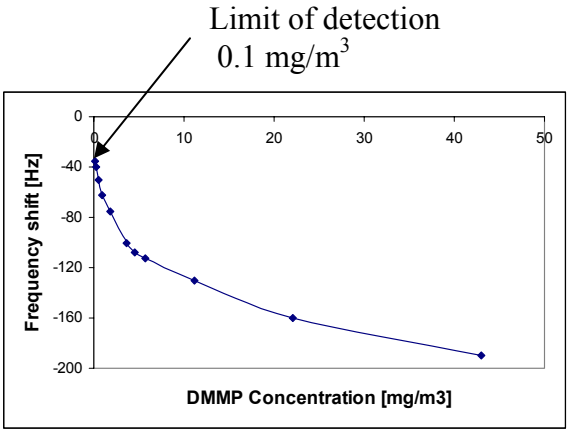


Fig.5. Cantilever response upon exposure to DMMP concentrations varying from 43 mg/m$^3$ to 0.1 mg/ m$^3$. The detection limit is 0.1 mg/m$^3$.

# MEMS-based Magnetometer Manufactured in 0.35μm SiGe BiCMOS Process

**Eli Richards and Dennis Wickenden**

***The Johns Hopkins University Applied Physics Laboratory, 11100 Johns Hopkins Road, Laurel, MD 20723***

***443-778-5338***

***Fax: 443-778-1313***

***Eli.Richards@jhuapl.edu***

# Prototype Magnetometers: CuBe and PolySi

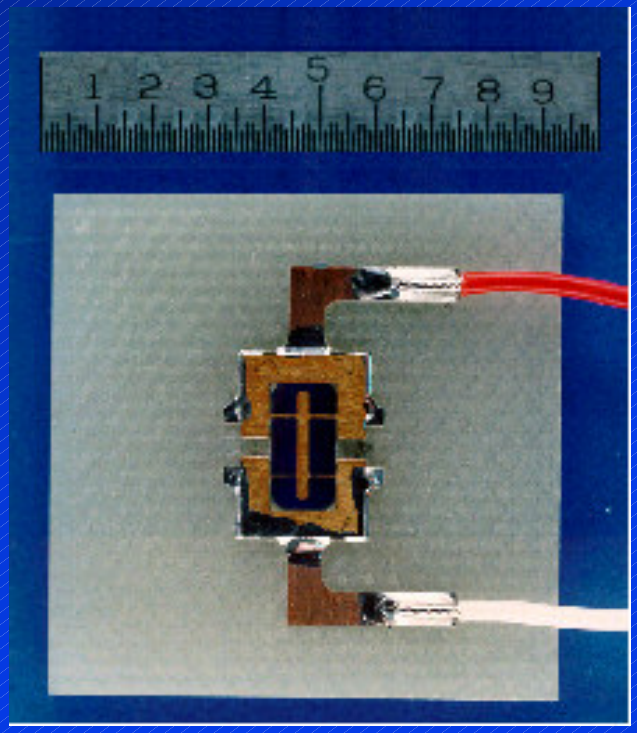


**CuBe Xylophone Bar**
**Fabricated at JHU/APL**

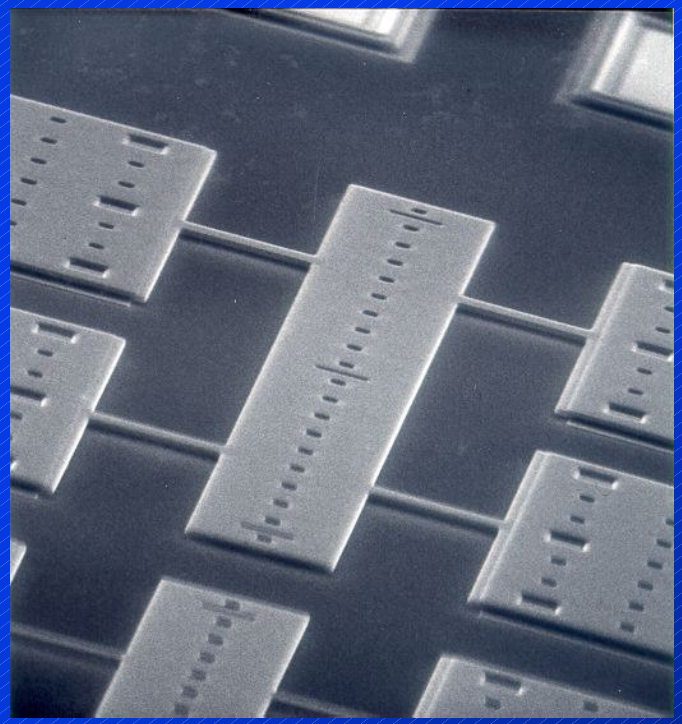

**PolySi MEMS Device**
**Fabricated at MCNC (Now MEMSCAP MUMPs Service)**

**Wireless Communications Systems for MEMS Sensor Arrays**

Matthew G. Bevan, Wolfger Schneider, Kenneth Wright
The Johns Hopkins University – Applied Physics Laboratory
11100 Johns Hopkins Rd., Room 13-N224
Laurel, MD 20723
Tele.:240-228-8944/Fax:240-228-6914
Matthew.Bevan@jhuapl.edu

One of the most promising applications for MEMS sensors is to use them in arrays to map the distribution of an environmental property. One challenge with creating networks of MEMS sensors is the communication infrastructure. If there are no space, power or wiring constraints, there are a number of communication protocols that can be employed; however, in an environment where excessive size and wiring interferes with the environment, the communications options become much more limited. Many organizations are developing new technology and new communication protocols to support these needs. We examined numerous communication protocols and their hardware implementation for an avionics application where numerous sensors are communicating with a central base station using a wireless communication link. We looked at protocols that would support IR and RF transmission, examining the data transmission efficiency, maximum data rates, power consumption and packaging requirements for communications systems using protocols such as Ethernet, Bluetooth and IrDA. Our results show that the optimum design is very sensitive to data transmission rates, transmission distance and the number of transmitting sites. Some of the protocols have limited hardware availability that curtails their use. It is important to understand the interaction of these factors with the protocol selection process.

There are a number of critical parameters in the design process, many of which are interrelated. The typical brute force approach solution used for a wired solution is inappropriate for a power-limited wireless environment. Sensor arrays provide unique challenges in that each station may be transmitting data collected at a slow rate, but when organized into an array of 100 or 1000, the base station may need to operate at a very high data rate. The protocols to support these high rates at the base station increases the requirements of the sensor nodes. (I.e. The need for the base station to operate at 10 Mbytes/s drives the sensor nodes to operate at the same speed even if they need to transmit data at only 10 Kbytes/s.) As the data rates go up and the communication range increases, the power requirements increase. Data overhead strongly drives system performance. As the overhead decreases, the data transmission time decreases leading to decreased power consumption. A critical measure of performance in this environment is power/data-byte which includes the data overhead as well as the power requirements.

# DESIGN AND PACKAGING CONSIDERATIONS FOR A MICROELECTROMECHANICAL SATELLITE THERMAL CONTROL DEVICE

Matthew A. Beasley, Samara L. Firebaugh
Electrical Engineering Department
United States Naval Academy
Maury Hall, Mail Stop 14B
Annapolis, Maryland 21403
Phone: (410) 293-6175
Fax: (410) 293-3493
Email: m040414@usna.edu

Richard L. Edwards, Allen C. Keeney and Robert Osiander
Johns Hopkins University Applied Physics Laboratory

**Abstract.** Trends in space technology require future satellites to be smaller and cheaper than their contemporary counterparts. This focus on optimizing mass has lead to the creation of micro and nano satellites down to the tens of kilograms. This new direction also requires a similar evolution in thermal control. Previous techniques such as heat pipes and conventional radiators have large masses themselves and are also not scaleable to fit these smaller designs. Microelectromechanical Systems offer unique advantages in mass and scalability. By coating a satellite with thousands of MEMS devices, thermal control can become responsive to fluxuations in thermal capacity.

The John Hopkins University Applied Physics Laboratory has been working on developing MEMS technology for small satellite thermal control for the past decade. Previous work has been done to create devices that use louvers or shutters to switch between two levels of emissivity. By mechanically altering the emissivity of devices placed on the exterior of the satellite, the heat flow from the satellite into space can be controlled. This in turn, allows the satellite to remain within its operating temperature range.

This project describes a variable radiator that relies on the heat conduction between the satellite and an external high emissivity film. The operating principle is illustrated in figure 1. This device uses a coated gold membrane as the suspended emissivity layer. Supporting the membrane are 2 μm high posts made of the photoresist polymer, SU-8. A cross section of the device is shown in figure 2. SU-8 has a low thermal conductivity, and therefore insulates the satellite when the device is off. Beneath the SU-8 posts is a thin layer of silicon nitride and the silicon substrate itself. The substrate would then be fixed to the exterior of the satellite. With the electrically isolating layer of silicon nitride between them, a capacitive force is produced. These devices were designed to operate at a voltage of 20 to 24 Volts, which is the bus voltage for many satellites in production today. We have achieved actual voltages of 18 to 30 V with prototype devices. This voltage is applied to an array of devices shown in figure 3.

Both electromechanical modeling and thermal modeling has been conducted. Initial testing confirms the electromechanical model. Future testing will focus on the thermal properties of the device. A redesign of this device is also being undertaken with thermal requirements in mind.

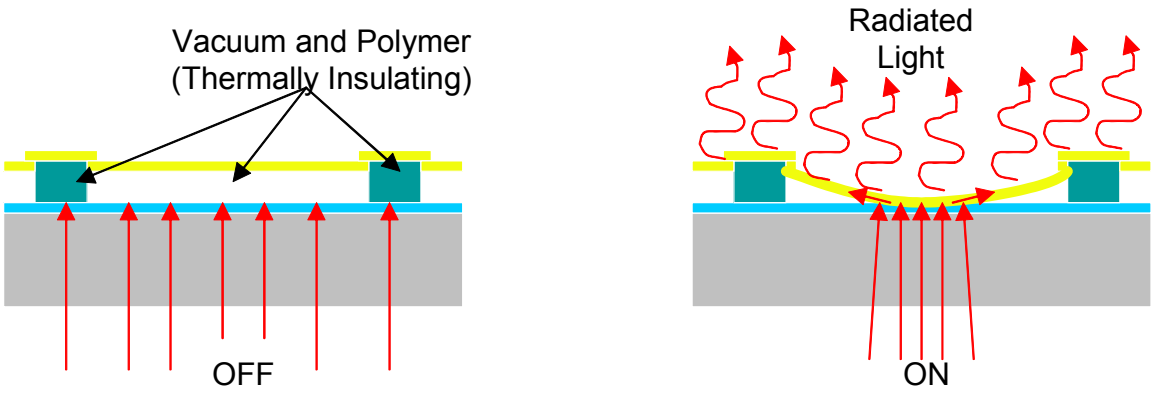


**Figure 1 Device operation principle.**

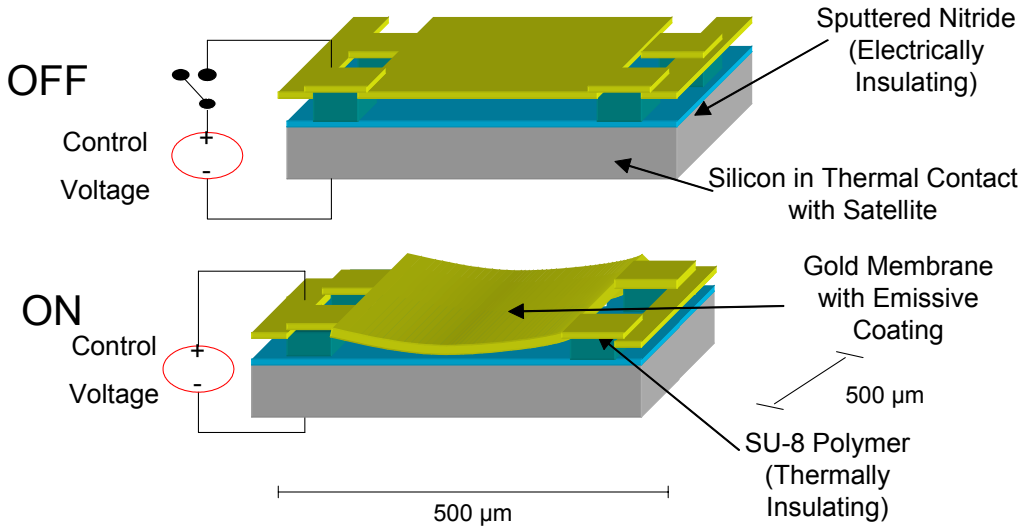


**Figure 2 Device cross section and design parameters**

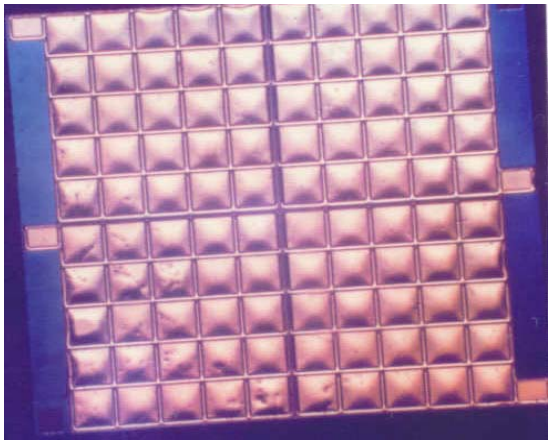

**Figure 3 Picture of MEMS device arrays.**

# Fuel-Air Mixing Challenges in Micro-Power Systems

Kiran Dellimore[1] and Christopher Cadou[1]

[1] Department of Mechanical Engineering, University of Maryland, College Park, MD 20742

Tel: 301.405.0829, Fax 301.314.9001, cadou@eng.umd.edu

## ABSTRACT

The high energy density of hydrocarbon fuels make them well-suited for storing energy on Micro Air Vehicles (MAVs) currently being developed for a variety of homeland security applications. One of the challenges faced by hydrocarbon fuel-based power systems is achieving good fuel-air mixing, however the nature of the challenge is unclear as the Reynolds number range in which mixing is expected to occur is not really known. A simple model based on the well-established 'jet in a cross-flow' (see figure 1) has been developed to predict this range as a function of overall size and power output. The model is explained and results are presented. An example of these results is presented in figure 2. It shows that flows in micro-power systems can span a very broad range with Reynolds numbers spanning the laminar, transitional, and fully turbulent regimes. The figure also shows, however, that Reynolds numbers associated with micro-power systems should be expected to be much smaller than in their conventional-scale counterparts. This suggests that achieving adequate fuel-air mixing will be more difficult than in conventional-scale power systems. Moreover, a survey of the literature indicates that there may be an absence of appropriate data in the appropriate Reynolds number range. As a result, predicting the performance of micro-scale fuel-air mixers may prove difficult and additional mixing studies may be required.

*2004 MEMS Alliance Symposium on MEMS in Homeland Security, Defense and Aerospace Applications*
*March 29-March 30, 2004*

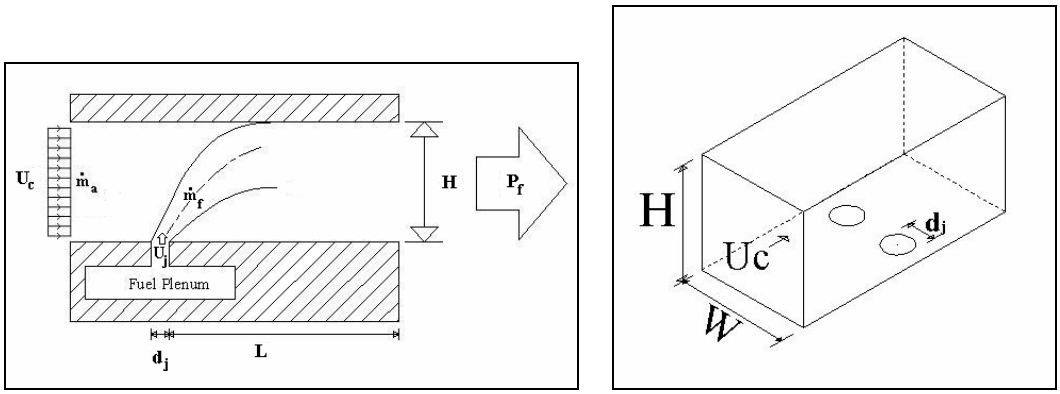


Figure 1. Illustration of a generic 'jet in a cross-flow' mixing configuration implemented in a rectangular micro-channel of height H and width W.

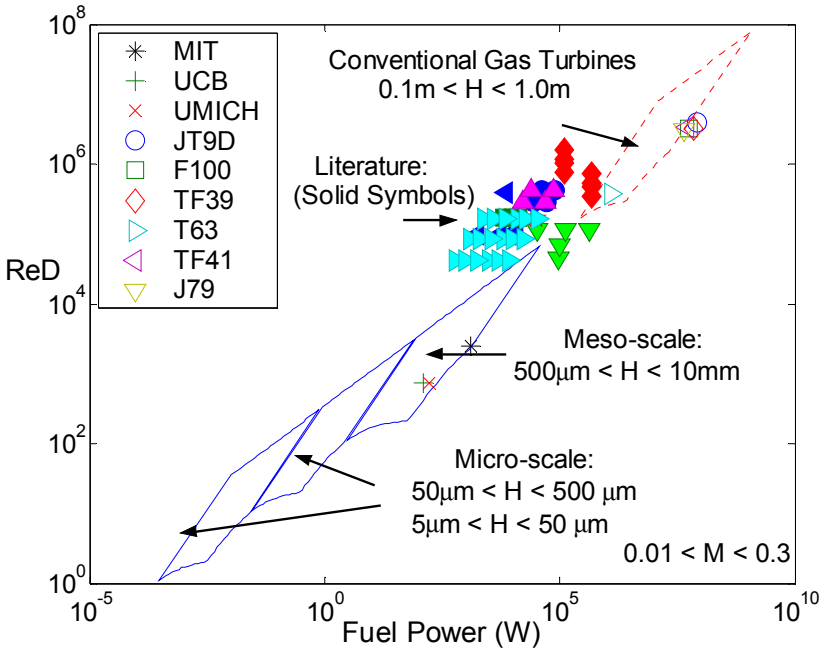


Figure 2. Crossflow Reynolds numbers associated with fuel-air mixing as a function of power associated with complete combustion of fuel. The first three symbols correspond to various micro-engines in development, the remaining open symbols correspond to various gas turbine engine combustors, and the solid symbols correspond to previous experimental investigations of gas-gas mixing

**Development of MEMS-based Micronozzles for Gas Separation**

Sheng Li[(1)], Carl B. Freidhoff[(2)], Robert M. Young[(2)], and Reza Ghodssi[(1)]
[(1)] MEMS Sensors and Actuators Lab (MSAL)
Department of Electrical and Computer Engineering
The Institute for Systems Research
University of Maryland, College Park
[(2)] Northrop Grumman Electronic Systems Inc.

Chemical sensors have been downsized over the past years due to advances in microelectronics and Microelectromechanical Systems (MEMS) technologies. The miniaturized chemical sensors have potential advantages of fast response, low power consumption and measurement of small flows. However, their sensitivity levels are still recognized to be too low for many applications such as cargo and personnel monitoring at commercial airports. MEMS-based micronozzles can be used as real-time preconcentrators for miniature sensors to enhance their sensitivities significantly. Here we report the design and fabrication of microscale linear and separation nozzles using anodic bonding and deep reactive ion etching (DRIE) techniques. The linear converging-diverging nozzle, as shown in Figure 1, is used to study fundamental gas dynamics in microfluidic devices. The fabricated nozzles are packaged to interface with a gas flow test setup that is developed to measure gas flow rates and pressure distributions in the micronozzles[1]. Figure 2 shows the effects of downstream pressure on the mass flow rate for a nozzle with a 10.9 μm wide throat and a 1.69:1 expansion ratio. According to compressible fluidics[2], the saturated gas flow rate demonstrates that a sonic gas flow is generated at the throat of the nozzle. In addition, gas flow tests are conducted to estimate viscous effects in micronozzles. As shown in Figure 3, the mass flow efficiency (i.e., the ratio of actual mass flow to the theoretical mass flow) is measured to vary from 0.43 at a Reynolds number of 62 to 0.81 at a Reynolds number of 262. This quantifies the blockage associated with the boundary layer[3], which becomes relatively thicker due to the increase in viscous losses at lower Reynolds numbers. These measurements and developed techniques form a basis for the design and fabrication of a separation nozzle shown in Figure 4, which consists of a curved converging-diverging nozzle, a skimmer, an inlet port and two outlet ports. This device is expected to concentrate heavy gas molecules of interest and to act as a front-end to enhance the sensitivity of a miniaturized chemical sensor. The detailed fabrication process and testing results will be presented.

References:

1. S. Li, C. B. Freidhoff, R. M. Young, and R. Ghodssi, "Fabrication of micronozzles using low-temperature wafer-level bonding with SU-8," *J. Micromech. Microeng.,* no. 13**,** 2003.
2. P. H. Oosthuizen and W. E. Carscallen, "Compressible Fluid Flow," (New York: McGraw Hill), 1997.
3. R. L. Bayt and K. S. Breuer, "Viscous effects in supersonic MEMS-fabricated micronozzles," Proceedings of the 3rd ASME Microfluids Symposium, Anaheim California, Nov. 1998.

Contact Author: Reza Ghodssi
Department of Electrical and Computer Engineering, University of Maryland, College Park, MD 20742
Phone: (301) 405-8158 Fax: (301) 314-9281 E-mail: ghodssi@eng.umd.edu

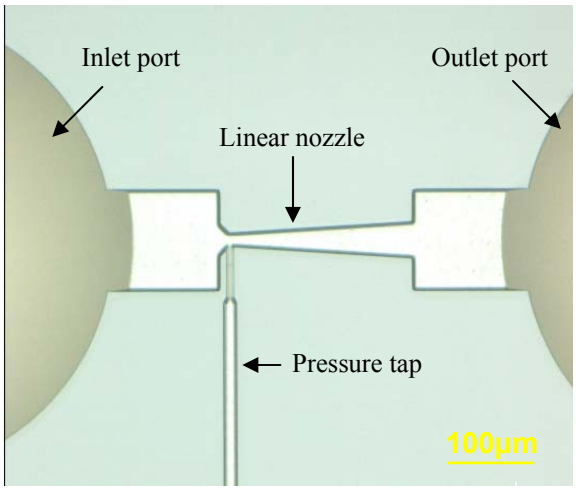


**Figure 1.** A microscope image of the bonded linear converging-diverging nozzle.

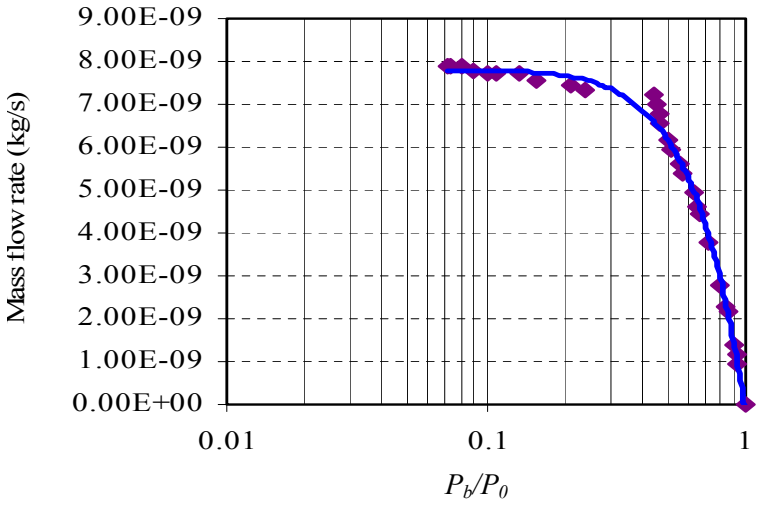


**Figure 2.** Effects of downstream pressure $P_b$ on the mass flow rate. The upstream pressure $P_0$ is kept at one atmosphere while the downstream pressure $P_b$ varied.

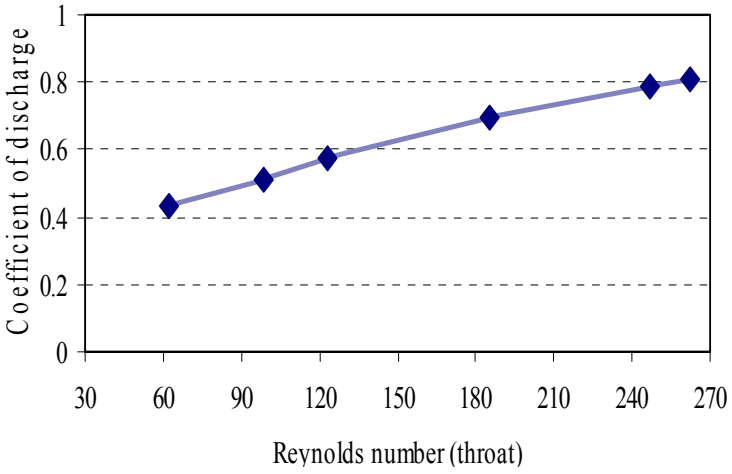


**Figure 3.** Variation of mass flow efficiency of the gas flow as a function of Reynolds number.

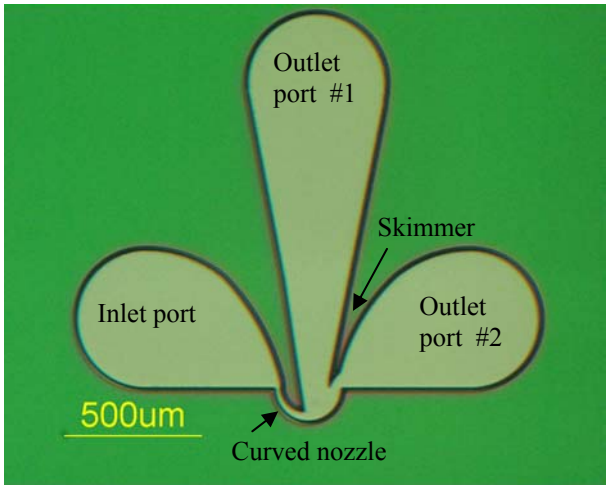


**Figure 4.** Micrograph of the separation nozzle structure etched in silicon substrate.

TITLE: Novel MEMS Stirling Cooler

AUTHORS: Keith J. Rebello, Matthew E. Moran, Danielle Wesolek, Bruk T. Berhane, and Ann Garrison Darrin

CONTACT:

Keith J. Rebello
The Johns Hopkins University Applied Physics Lab
11100 Johns Hopkins Road
Mailstop: 2-217
Laurel, MD 20723
Tel: 240-228-7158 (Washington)
443-778-7158 (Baltimore)
FAX: 443-778-6904
E-mail: keith.rebello@jhuapl.edu

ABSTRACT:

Electronic subsystems for military and aerospace applications can generate large amounts of heat. Removal of this waste heat is a major challenge for system engineers and greatly limits device performance. Novel and active thermal management systems are required to enable high levels of efficiency and high power densities in small physical form-factors. This is true for both discrete devices and for integrated circuits such as microprocessors and digital signal processors. Passive cooling techniques may not be viable for many applications. This presentation will cover a patented microsystem Stirling cooler with a predicted efficiency of 30% of Carnot which is currently under development with potential uses in electronics, sensors, optical & RF systems, microarrays, and other microsystems. The microsystem Stirling cooler is most suited to volume limited applications that require cooling below the ambient or sink temperature. Primary components of the planar device include: two electrostatic comb-drive diaphragm actuators that replace the pistons found in macro-scale Stirling machines, and a micro-regenerator that stores and releases thermal energy to the working gas during the Stirling cycle. A comparison of three candidate micro-regenerators was performed. The candidate regenerators were tested in a custom piezoelectric-actuated test apparatus. Results of the evaluations of these MEMS components will be presented. The MEMS diaphragm actuators are presently being fabricated and an analysis of their design will be presented. This MEMS Stirling cooler has the potential to out perform other methods in constrained critical end item applications.

**Fabrication of MEMS-Based Microshutter Arrays for Optical Transmission Selection**

Bernard A. Lynch[1] and David E. Franz, R.G. Hu, M.D. Jhabvala, C.A. Kotecki, M.J. Li, H. Oh, Y. Zheng

[1]NASA Goddard Space Flight Center, Greenbelt, MD 20771, USA
Phone: 301.286.3599; Fax: 301.286.1672
e-mail: bernard.a.lynch@gsfc.nasa.gov

A MEMS-based programmable aperture mask is under development at the NASA Goddard Space Flight Center. Termed the Microshutter (μ-shutter) Array, the device will be used to control the transmission of light, with both high efficiency and contrast, to a multi-object spectrometer on the James Webb Space Telescope. Fabrication of the μ-shutter array employs several novel designs and processing techniques. The current generation of μ-shutters consists of 128x64 pixel arrays with unit cell dimensions of 100x200 μm. Shutters are patterned in silicon nitride and sit on a 100 μm silicon frame that is DRIE etched below each shutter. The front and back sides of the device are shown in Figure 1. A magnetic cobalt-iron alloy patterned on top of the shutter allows it to be actuated 90˚ out-of-plane, into the frame, by an external magnetic field. An electrode on the shutter and a vertical electrode on the sidewall of the frame, approximately 90μm deep, allow them to be electrostatically latched in their rotated position. The vertical electrode is deposited and patterned on the backside of the frame in a single step using a directionally controlled evaporation. Individual addressing of shutters for electrostatic latching is accomplished via a crosspoint addressing scheme, with no on-chip active components. Figure 2 shows a portion of an array with shutters in the open, latched, and closed positions. Light loss at shutter edges is minimized by an overhanging aluminum light-shield that is anchored to the frame, as shown in Figure 3. A photoresist sacrificial layer is used to raise the light-shield up and over the 2 μm gap that surrounds each pixel. After completion, arrays are subjected to life cycle, environmental and optical testing. Fabricated devices have survived $10^6$ actuation cycles at both room and cryogenic temperatures and a 14g rms launch-simulation test. Optical testing has shown contrast measurements between open and closed shutters up to 10000:1.

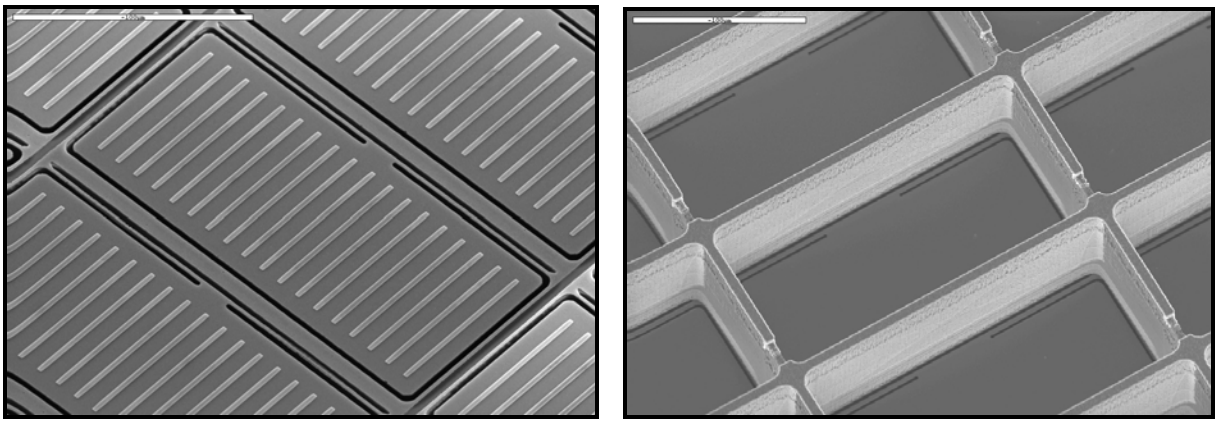

**Figure 1 Images of the front and back sides of the μ-shutter array.**

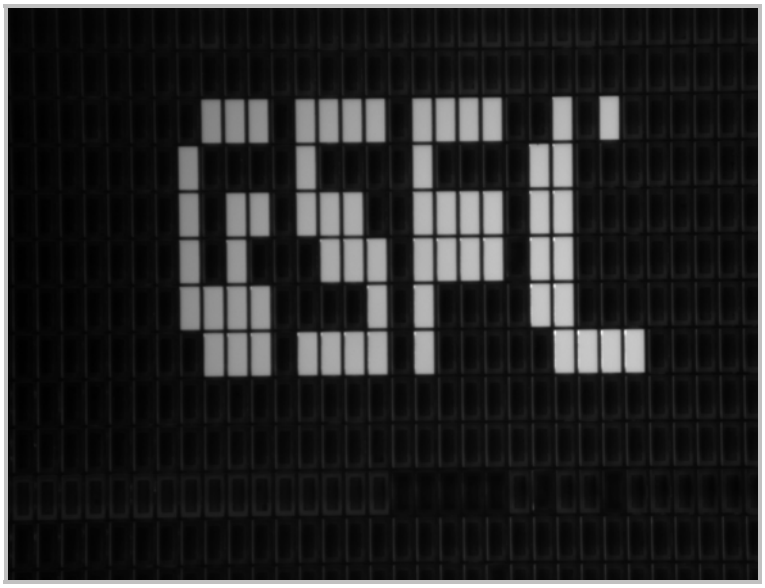

**Figure 2 μ-shutter array with 2-D addressing. Light areas indicate open shutters.**

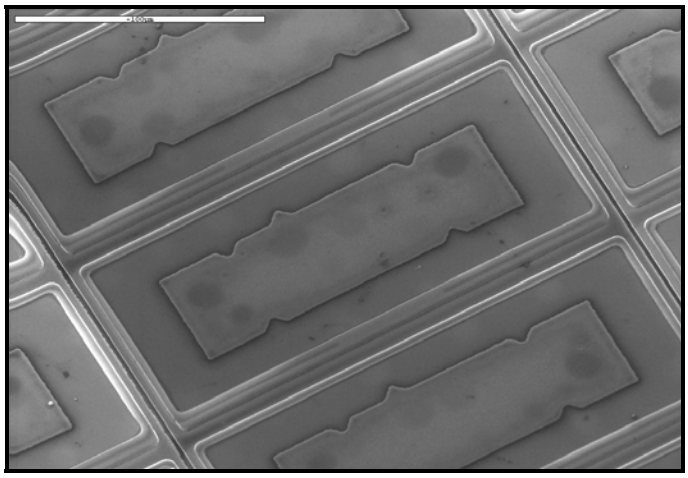

**Figure 3 SEM image of several shutters with integrated light-shield.**

# A Micro-machined Flat Plasma Spectrometer (FlaPS)

Danielle M. Wesolek[*a], John L. Champion[a], Fred A. Hererro[b], Robert Osiander[a], Roy L. Champion[c] Ann M. Darrin[a]
[a]The Johns Hopkins University Applied Physics Laboratory, 11100 Johns Hopkins Road, Laurel, MD, USA 20723;
[b]NASA Goddard Space Flight Center, Code 692, Greenbelt, MD, USA 20771;
[c]The College of William and Mary, Williamsburg, VA, USA, 23187

## ABSTRACT

The trend toward deploying constellations of ever-smaller spacecraft, including nanosats and picosats, for characterizing the magnetosphere will require new miniaturized plasma spectrometers with a high ion throughput to instrument volume ratio. Through a new approach to energy analysis, to microelectromechanical systems (MEMS), the Flat Plasma Spectrometer (FlaPS) presented here provides solution to the investigation of plasma distributions in space. It is capable of measuring the kinetic energy and angular distributions of ions/electrons in the space environment for energies ranging from a few eV to 50keV. A single pixel of a FlaPS instrument has been designed, built and tested to occupy a volume of approximately one cubic centimeter, and is characterized by a high throughput-to-volume ratio, making it an ideal component for small-scale satellites. The authors achieve significant reductions in mass and power for a given geometric factor, plus energy selectors with larger energy/voltage ratios. The new approach can afford to abandon energy focusing with the aid of the new collimator technology. It still measures energy just as easily; perhaps more easily because, for a given electron or ion energy, the required voltage is about $1/10^{th}$ the voltage required in conventional spectrometers. One key to miniaturization here lies in the collimator array that the ions or electrons must pass before entering the energy selector array. The front end of the prototype instrument was fabricated using advanced micro-fabrication techniques, and consists of a collimator, electrostatic analyzer, drift region, and an energy selector mask. Below that is a matched pair of micro-channel plates (MCP) and anode for amplification and detection. To illustrate the basic concept, ion trajectory simulations were performed to calculate/simulate the path of selected particles, and experimental measurements were obtained as proof of concept for analyzing ion energies. This novel instrument concept will yield an enabling technology for constellations of small satellites where minimizing factors such as weight and cost are crucial.

[*]Electronic mail: Danielle.Wesolek@jhuapl.edu ; phone 443-778-8903; fax 443-778-6904

2004 MEMS Alliance Symposium on MEMS in Homeland Security, Defense and Aerospace Application
March 29-March 30, 2004

# Effect of Structural Heat Conduction on Flame Propagation and Power Density in Micro-Combustors

Timothy Leach[1], Christopher P. Cadou[2], and Gregory S. Jackson[3]

[1] Department of Aerospace Engineering, University of Maryland, College Park, MD 20742

Tel: 301.405.0829, Fax 301.314.9001, cadou@eng.umd.edu

[2] Department of Mechanical Engineering, University of Maryland, College Park, MD 20742

## ABSTRACT

The performance of millimeter-scale combustors that have applications in the development of compact propulsion systems for micro-air vehicles is strongly influenced by heat exchange to and within the combustor structure. A simple one-dimensional model for the effect of structural heat exchange on the propagation of a flame in a conductive duct has been developed. The model is an extension of the well-established thermal theory of flame propagation by Mallard and Le-Chatelier that include heat exchange between the gas and structure as well as within the structure itself. The model shows that the reaction zone thickness (or the burning rate) starts to increase when the height of the passage falls below a critical value. The critical passage height at which this transition begins depends on the Nusselt number for heat transfer between the gas and the structure. The reaction zone thickness (or burning rate) continues to increase as passage height is reduced until another limit is reached. This limit is set by the thermal conductivity of the combustor wall. These results are consistent with the effects of pre-heating the reactant mixture in conventional-scale flames. Including heat loss to the environment introduces a third limit in which the flame extinguishes (or quenches) if the passage height is made too small. Figure 1 shows that the predictions of this remarkably simple model compare favorably with a more complete one-dimensional numerical simulation of the reacting fluid flow that includes full chemistry, distributed heat exchange between the reacting gas and the structure, and heat exchange within the structure itself. The reference length scale in the figure is $\delta_{r,fr}$ , the thickness of a freely propagating flame. Finally, it is important to note that while continuum-based models are used for the fluid, thermal slip at the wall is accounted for so that the model and simulation predictions remain valid for passage heights that fall well into the slip regime.

The model and simulation are used to study the effects of axial heat transfer from the post-flame to the pre-flame via wall conduction in a silicon micro-channel combustor with planar symmetry. They show that axial heat transfer widens stability limits, increases the burning rate, and can enable the construction of smaller, higher power density combustors. Figure 2, which shows contours of power density and efficiency as a function of passage height and passage length indicates that achieving high power density comes at the expense of achieving high efficiency. The simulations also show that heat loss to the environment places a lower bound on the combustor volume. Increasing the pressure in the combustor increases its power density while the micro-channel length and height associated with the maximum tend to decrease.

*2004 MEMS Alliance Symposium on MEMS in Homeland Security, Defense and Aerospace Applications*
*March 29-March 30, 2004*

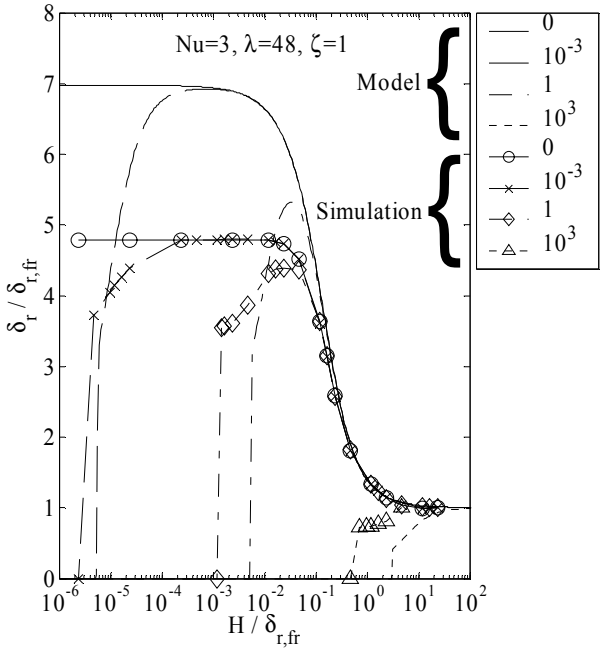


Figure 1. Fractional increase in reaction zone length $\delta_r$ as a function of the normalized flow passage height $H/\delta_{r,fr}$ for a range of heat transfer coefficient in $W/m^2K$. Solid lines correspond to the analytical model and the symbols correspond to numerical model results. The mixture is $H_2$-air at an equivalence ratio of 1.

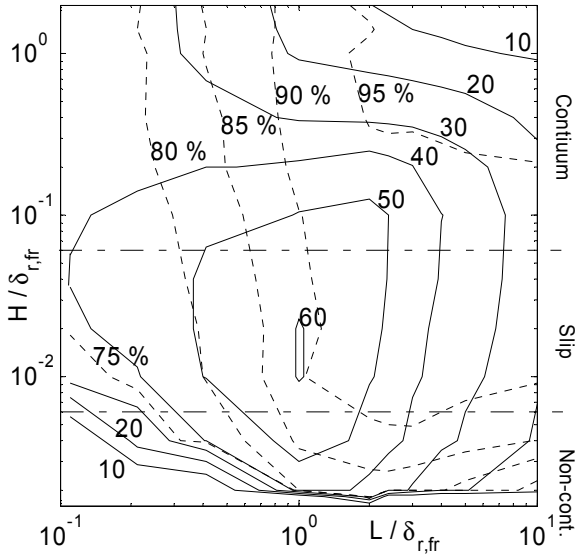


Figure 2. Non-adiabatic $H_2$-air combustion in a silicon micro-channel; $\Phi$=0.5, $P$=1atm, $h_{env}$=1 $W/m^2K$. Solid lines: Contours of non dimensional power density $\left(\dot{w}_D/\dot{w}_{D,ref}\right)$ as a function of non-dimensional channel height and length. Dashed lines: Contours of overall efficiency. Dash-dotted lines: boundaries between continuum, slip, and transition regimes.

**Shear Stress Sensors for Turbulence Control**

Sateesh S. Bajikar[1], Michael A. Scott[2] and Edward E. Adcock[2]

[1]NASA Goddard Space Flight Center/QSS, [2]NASA Langley Research Center

Bldg.11, E032, Org. Code: 553
NASA, Goddard Space Flight Center
Greenbelt, MD 20771
301.286.4457
Fax: 301.286.1672
Sateesh.Bajikar@gsfc.nasa.gov

**Abstract**

Sensors for measuring wind shear stress or drag forces are under development in a collaborative effort between GSFC and LaRC. Such sensors are expected to play a crucial role in understanding and controlling the onset of turbulence in flow in aerodynamic and hydrodynamic situations. MEMS technology is well suited for meeting many of the requirements for such sensors. This poster presentation will illuminate the performance and other requirements and the unique challenges such sensors present. It will also showcase the results of the work to date, chiefly the design and fabrication of a "fence-type" design sensor device.

**Title:**

Interferometric Optical Detection in a Silicon on Sapphire CMOS Process

**Authors:**

Francisco Tejada (Student)*
Email: ft1@jhu.eu

Andreas G. Andreou *
Email: andreou@jhu.edu

*The Johns Hopkins University
Dept. of Electrical and Computer Engineering
3400 N Charles Street
105 Barton Hall
Baltimore, MD 21218
Tel: 410 516 8361
Fax 410 516 2939

Joseph A. Miragliotta +
E-mail: joseph.miragliotta@jhuapl.edu

Robert Osiander +
E-mail: robert.osiander@jhuapl.edu

+The Johns Hopkins University
Applied Physics Laboratory
11100 Johns Hopkins Road
Laurel, MD 20723
tel: 443-778-6247
fax: 443-778-6904

**Presentation:**

Poster

**Abstract**

Sensing MEMS motion through capacitive sense techniques is the industry standard and is employed in many commercially available devices such as Analog Devices accelerometers and gyroscopes. However, structural constraints are imposed in this sensing method, making it practical for measurement of displacement in the plane. Optical detection methods allow for the design of simple and optimized mechanical structures, not hampered by the necessity of incorporating capacitive sense fingers, and have the potential for higher sensitivity. Integration of readout sub-systems in standard CMOS technology is however difficult as most structures are not compatible with standard CMOS processing.

Perergrine Semiconductor's ultra-thin silicon (UTSi) on sapphire CMOS process (SOS-CMOS) gives a transparent substrate that allows for the design of hybrid and compact optical detection systems that can be implemented at the chip scale. Two types of interferometers are considered for the envisioned optical readout architecture (fig. 1). Both systems utilize commercially available vertical cavity surface emitting lasers (VCSEL) as the light source. The MEMS device can be fabricated in any process so long as the top surface is reflective. The design of the detector structures and associated electronics on the SOS-CMOS die determines the type of interferometric detection system that can be fabricated.

The Fabry-Perot type interferometer has been implemented in the macro scale on an optical bench (fig.2).A Hitachi laser diode is used instead of a VCSEL. The wavelengths of the VCSEL and laser diode only differ by ten nanometers. A piezo-actuated mirror is used to simulate the MEMS device motion. The mirror is sent a .1mV AC sine wave at 1 kHz from the function generator, so the lock-in amplifier can detect the signal. The DC offset of this sine wave is then increased linearly so the mirror moves closer to the photodiode. Standing wave interference is seen in a 200 μm square PIN SOS photodiode (fig.3).

The first step in the hybrid integration of the system is flip chip bonding the VCSEL to the CMOS-SOS die. The MEMS device is also flip chip bonded to the sapphire plate.
Next the combined VCSEL CMOS-SOS parts are attached to the combined MEMS sapphire slide plate parts with an index matching fluid. The index matching fluid serves a dual purpose, it mechanically attaches the CMOS-SOS die to the sapphire slide and it provides better optical transparency by filling the asperities on the bottom surface of the CMOS-SOS die. Another advantage of using the index matching fluid to join the SOS with the PolyMUMPS is that it can be reflowed and the SOS die can be recovered and reused many times. The fully assembled device is then packaged as needed; some MEMS devices require a hermetic seal while others need only vacuum.

Currently we have assembled the components necessary for the final architecture. An SOS CMOS die was fabricated in December of 2002. We have successfully bonded the sapphire plate to the MEMS die, and have bonded the VCSEL to the SOS CMOS die (fig. 4). This VCSEL to SOS bonding requires more development as it is difficult to exert the small forces needed. If the force is to great then the ball bonds for the VCSEL are smashed together therefore shorting out the connections.

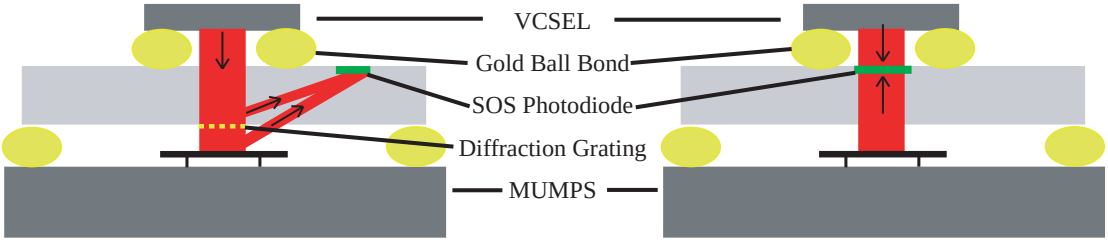

Figure 1: Cross sectional view of the detection architctures

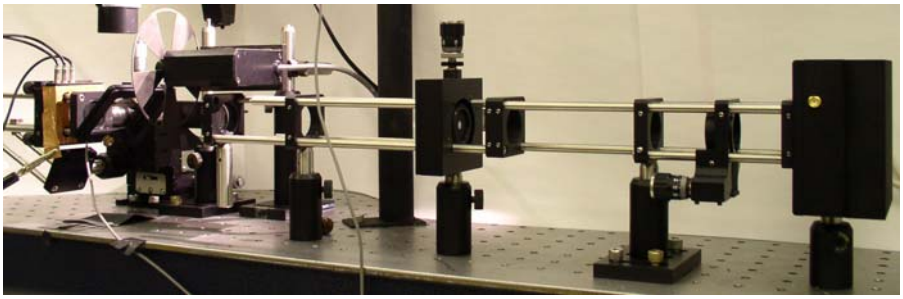
Figure 2: Picture of Fabry-Perot optical bench test setup

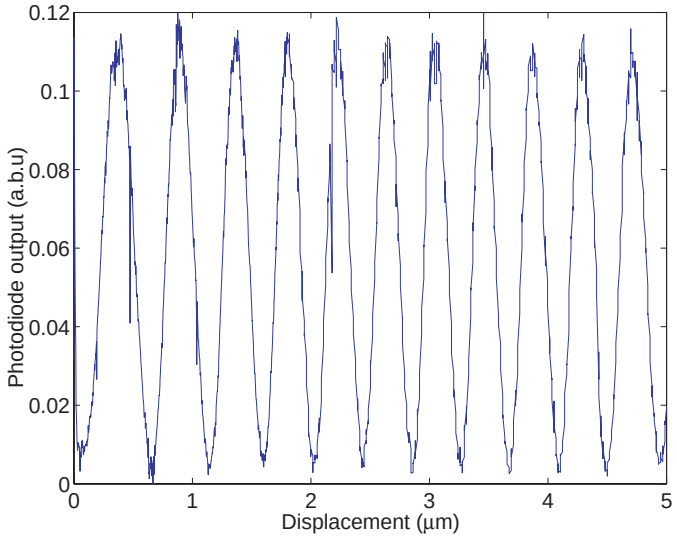

Figure 3: Experimental data showing interference in PIN SOS photodiode

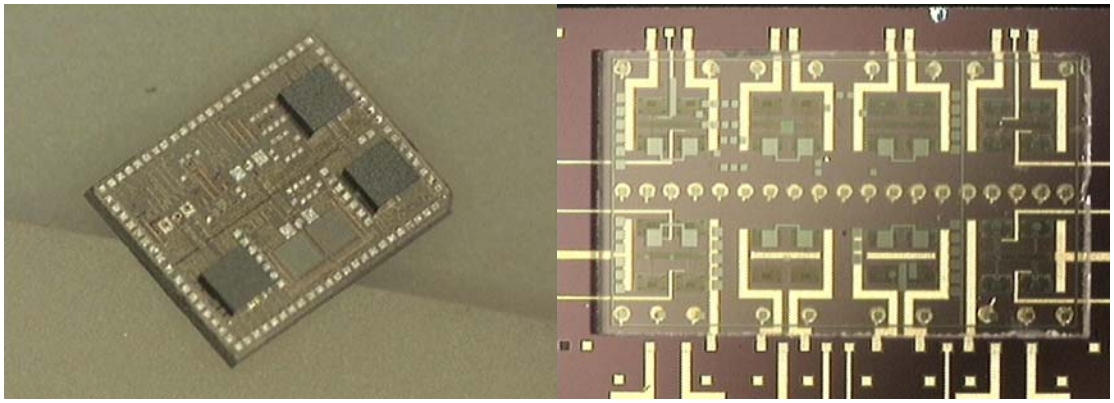
Figure 4: VCSEL bonded to SOS(left) and Sapphire Plate bonded to MUMPS die(right)

# MEMS TACTILE ACTUATORS FOR PILOT ORIENTATION SYSTEMS

James E. Smith, John D. Roth, Samara L. Firebaugh
Electrical Engineering Department
United States Naval Academy
Maury Hall, Mail Stop 14B
Annapolis, Maryland 21403
Phone: (410) 293-6175
Fax: (410) 293-3493
Email: m045934@usna.edu

Currently tactile actuators are used in flight suits to provide information to the pilot through the generally unused stimulus of touch. These actuators are pneumatically powered, large, and bulky. By replacing these actuators with MEMS technology they will become more convenient, consume less power, and produce less noise.

We have explored three methods of out-of-plane actuation implemented through the PolyMUMPS® process. The PolyMUMPS process is a shared user fabrication process that uses sacrificial micromachining to create suspended polysilicon structures. Two of our tactile actuator types use thermal actuation, and a third actuator type uses electrostatic force.

The first design is a bimetallic "U" shaped cantilever. The cantilever is heated by applying a voltage across its ends. Because the two metallic layers in the cantilever expand at different rates the lever is deflected upward. This method uses the gold layer in the PolyMUMPS process followed by an additional metal layer that we plan to deposit using electroplating.

The second actuator design again uses heat to gain the out-of-plane motion. Instead of using differences in thermal expansion of metals, this design is purely polysilicon. A voltage differential is placed across a bottom layer "U" which is affixed at the bend of the "U" to a strut attached to the substrate. Current through the "U" heats the U-portion of the structure, causing it to expand, push against the strut, and create useable motion.

Instead of heat, the third actuator utilizes comb drives. The comb drive is attached to a hinge that will transform the in-plane motion of the drive into useful out-of-plane motion. Unfortunately, to generate the forces necessary to be effective in a tactile interface, the design requires fairly high voltages that may pose a problem to anyone with one against their skin.

Finally, a study on tactile resolution was conducted to determine the operating parameters our tactile actuators must meet in order to accomplish our goal of tactile stimulation. Using a piezoelectric actuator we found the skin is most sensitive to vibrations at 250-300 Hz. In addition to this, sensitivity was found to be much greater on the fingers and palm than it was on the arm and other parts of the body. This poster will present our design for the different types of actuators and the results of our skin sensitivity tests.

*2004 MEMS Alliance Symposium on MEMS in Homeland Security, Defense and Aerospace Applications*
*March 29-March 30, 2004*

**Maskless Fabrication of JFETs via Focused Ion Beams**

Anthony J. De Marco, John Melngailis
University of Maryland Department of Electrical and Computer Engineering
Energy Research Building, University of Maryland, College Park MD 20742
Tel: (301) 405-0030 FAX: (301) 314-9437
Email: adeptus@wam.umd.edu

Focused ion beam (FIB) systems are commonly used in industry to repair and modify optical lithography masks via ion-enhanced etching and ion-induced deposition. These techniques have also been applied to the modification of interconnects within finished devices, and are most valuable in the design and testing stages of microcircuit manufacture, when the layout may need to be changed often to meet desired performance goals. This work investigates the next level of FIB circuit modification: the creation of active devices utilizing solely FIB fabrication. Direct-write transistor fabrication opens up a wide range of possibilities for device prototyping, and limited circuits fabricated on non-planar geometries where traditional lithographic processes would not work, such as in some MEMS devices.

FIB techniques were used to construct junction field effect transistors (JFETs) on a mesa of n-type silicon situated atop a layer of silicon dioxide. The device design is shown schematically in Figure 1, and an SEM image of a finished device is shown in Figure 2. Doping was conducted using a high energy FIB implanter to direct-write the desired dopant profiles. The source and drain regions were implanted using a beam of singly-charged arsenic ions accelerated to 120 kV. The gate was similarly implanted with singly-charged boron ions at 10 kV, with a dose that varied between $10^{14}$ ions per $cm^2$ and $10^{15}$ ions per $cm^2$ for different devices. The source, gate, and drain contacts were directly written by FIB as well, using a 30 kV gallium ion beam and an organo-metallic precursor gas to effect ion-induced deposition of conductive platinum compound. FIB deposited platinum forms an ohmic contact to heavily doped silicon, with an average contact resistance of $9.17 \times 10^{-3}\ \Omega \cdot cm^2$ as measured in previous work. The resistance of an individual contact can vary somewhat, and has been measured as low as $3.58 \times 10^{-3}\ \Omega \cdot cm^2$, which compares favorably to the contact resistance of Al-Si alloy contacts to comparably doped silicon, which is $10^{-4}\ \Omega \cdot cm^2$.

Several proof-of-concept devices were made to demonstrate the technique's potential; the current-voltage characteristics of one such JFET with FIB-fabricated dopants and contacts is shown in Figure 3. Some devices were created with evaporated aluminum contacts instead of FIB-platinum to provide more stable contacts, and allow for comparison of how FIB gate doping affects device characteristics. A graded doping profile was found to be an effective means of decreasing the short-channel effects that result in increasing source-drain current past saturation. The saturated drain-source resistance $R_{SAT}$ of the a JFET with a uniform $10^{14}$ $cm^{-2}$ doping profile and no gate bias was measured to be 2.25 MΩ. By contrast, for a JFET with a linearly graded doping profile from $10^{14}$ $cm^{-2}$ to $10^{15}$ $cm^{-2}$ near the drain $R_{SAT}$ is 21.9 MΩ. When voltage is applied to the source and the drain grounded, the effect is reversed and $R_{SAT}$ is reduced to 310 kΩ.

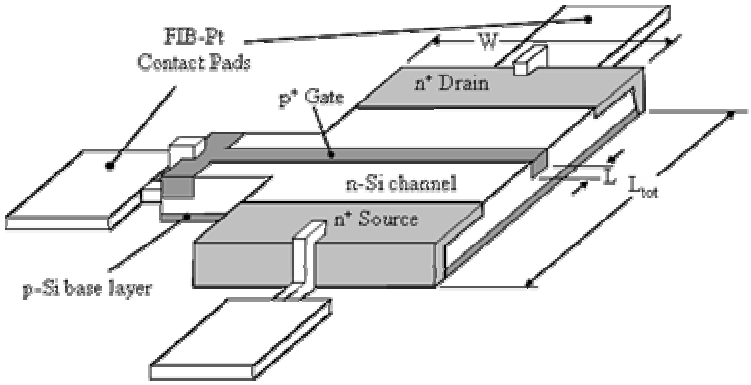


**Figure 1:** Isometric diagram of FIB-JFET, Si mesa constructed on SOI chip for device isolation. Device dimensions $L_{tot}$ and W are both 90 μm, gate length $L$ is1 μm.

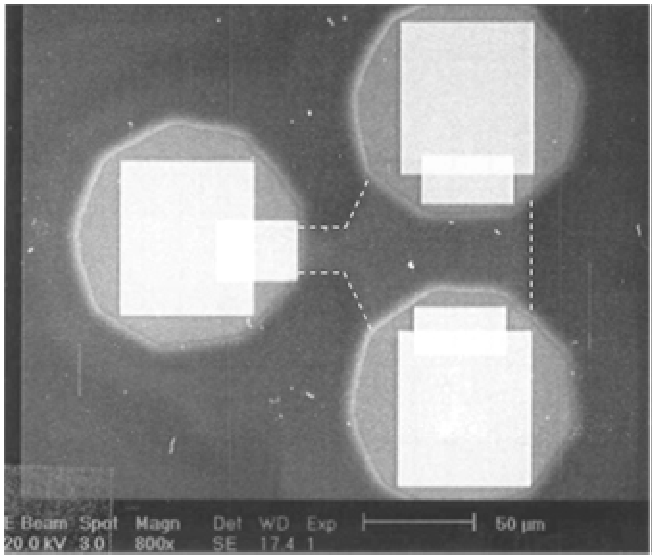


**Figure 2:** Top down SEM image of FIB-JFET. Bright areas are FIB-deposited Pt contact pads; artificial dotted lines denote the Si mesa seen through 200 Å of thermally grown surface oxide for device isolation.

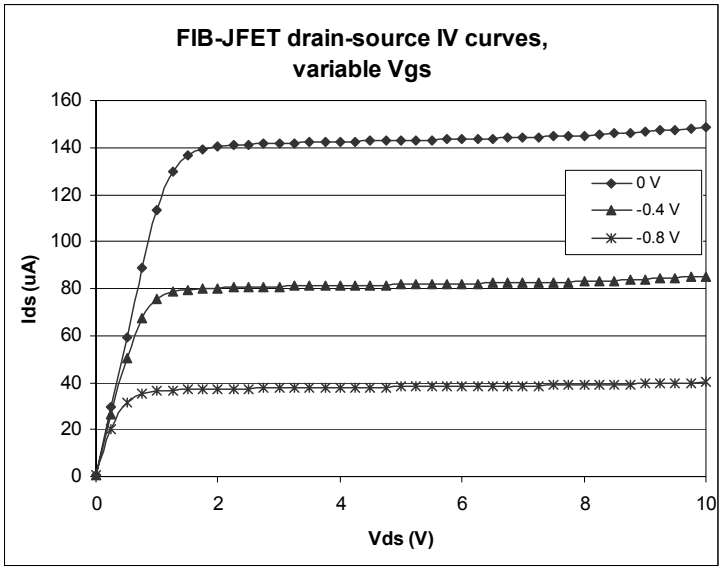


**Figure 3:** Current-voltage characteristics for FIB-JFET with uniformly doped 1 μm $p^+$ gate and FIB-deposited platinum contacts to the active area. $V_{DS}$ applied to drain, $V_{GS}$ applied to gate, source grounded.